Automation in Construction 180 (2025) 106569

Contents lists available at ScienceDirect

Automation in Construction

journal homepage: www.elsevier.com/locate/autcon

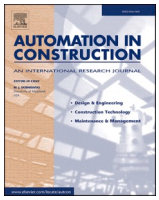

Exact optimization of surveillance camera placement in dynamic construction sites

Mohadeseh Farkhondeh, Mojtaba Maghrebi *

Department of Civil Engineering, Ferdowsi University of Mashhad, Iran

ARTICLE INFO

Keywords:
Camera placement optimization
Construction site monitoring
Dynamic construction environments
Optimization model

ABSTRACT

Surveillance camera systems are essential for construction monitoring tasks, including safety, productivity, progress tracking, and quality control. This paper investigates optimal design and dynamic adjustment of multi-camera systems across construction phases while minimizing cost. The problem is formulated as a Mixed-Integer Linear Programming (MILP) model that incorporates evolving layouts, relocation costs, camera specifications, and risk-based priorities. As construction progresses, new obstacles can affect coverage, and the approach includes camera replacement across phases. The method was evaluated on a real-world case study involving four construction phases, achieving a 17.64 % cost reduction while maintaining effective coverage of high-priority zones. These results provide construction managers with a practical decision-support tool for adaptive and cost-efficient surveillance planning in dynamic environments. Nonetheless, the model is currently limited to two-dimensional layouts, and its practical application depends on the availability of sufficient computational resources for solving the exact optimization problem.

1. Introduction

It is known that the construction industry is one of the most hazardous sectors, with an exceptionally high percentage of occupational injuries and fatalities reported [1–3]. In the United States, in 2019, 5333 worker fatalities occurred, 1061 of which were from the construction industry [4]. Similarly, it was reported that about 50 % of all job-related fatalities occur in the construction sector in Korea [5]. Many of these incidents are due to non-compliance with safety protocols and unsafe behaviors, such as failure to wear personal protective equipment (*PPE*) or using unsafe tools and procedures [6–8].

To mitigate such risks, camera-based monitoring systems integrated with computer vision technologies have received increasing attention as a promising tool for improving site safety through automated hazard detection [9]. These systems offer several advantages, including cost-effectiveness, non-intrusiveness, and continuous remote monitoring capabilities. However, beyond safety enhancement, surveillance cameras have become increasingly important in improving two other critical aspects of construction project performance: productivity and quality.

In terms of productivity, surveillance systems enable the continuous tracking of worker movements and machinery operations, offering valuable insights into task durations, idle times, and equipment utilization patterns. These data streams facilitate objective assessments of performance, identification of workflow inefficiencies, and proactive resource reallocation [10,11]. For quality assurance, high-resolution video feeds from strategically positioned cameras allow for real-time or post-event inspection of construction activities, material handling, and workmanship. This supports the early detection of deviations from design specifications—such as improper installations or surface defects—thereby minimizing costly rework and ensuring compliance with quality standards [12]. These multi-functional applications position surveillance cameras as a foundational element of modern construction management, offering real-time insights into safety, productivity, and quality performance indicators.

Despite the growing interest in vision-based monitoring, the strategic placement of surveillance cameras remains an unresolved challenge. The fixed positioning of *CCTV* units often leads to blind spots or redundant coverage. Therefore, it is imperative to ensure that cameras at construction sites are placed optimally for maximum effectiveness [13]. Surveillance effectiveness can be improved by aligning camera positions with a site's unique layout, hazards, and at-risk areas [14]. This can also enhance the overall safety of a construction site and minimize reliance on remote monitoring by experts or training-dependent personnel. Reducing this reliance helps lower the labor costs associated with

* Corresponding author.
E-mail address: mojtabamaghrebi@um.ac.ir (M. Maghrebi).

https://doi.org/10.1016/j.autcon.2025.106569
Received 7 September 2024; Received in revised form 18 September 2025; Accepted 25 September 2025
Available online 1 October 2025

traditional surveillance processes, which are prone to human error [9]. This motivates the formalization of the Surveillance Camera Placement Problem (*SCPP*), which aims to maximize effective monitoring coverage while minimizing camera count and cost [13–15].

While SCPP has been addressed in various domains, key challenges such as construction site dynamics, camera relocation costs, and avoiding excessive coverage of irrelevant areas remain largely unresolved or have been studied in isolation. Additionally, *SCPP* is classified as an *NP-hard* problem, which has led many researchers to rely on heuristic or metaheuristic algorithms that sacrifice global accuracy for computational speed [16,17]. Nevertheless, the proposed Mixed-Integer Linear Programming (*MILP*) formulation enables the identification of a global optimum under the defined constraints and bounded search space. This is achieved using exact solvers such as *CPLEX*, which employ branch-and-bound algorithms to identify the global optimal solution. It is important to emphasize that we do not claim polynomial-time solvability for all *NP-hard* problems. Rather, we emphasize that the inherent structured nature of our *SCPP* formulation facilitates exact optimization within feasible computational limits.

To address these gaps, this study introduces a dynamic and cost-aware optimization framework for *SCPP* based on Mixed-Integer Linear Programming (*MILP*). Unlike traditional static models, the proposed approach incorporates construction phase dynamics, risk-based monitoring priorities, and camera relocation costs into a unified mathematical formulation. The model ensures globally optimal placement decisions across all project phases, thereby achieving precise coverage of critical zones while avoiding unnecessary monitoring of irrelevant areas. Notably, the inclusion of a relocation-aware cost model provides an economic dimension that balances trade-offs between installing new cameras and reusing existing ones, making the method highly practical for budget-constrained projects.

Therefore, this study is guided by the following research question:

How can a surveillance camera system be optimally designed and dynamically adjusted across different construction phases to ensure effective coverage while minimizing total cost?

To address this, we introduce a MILP-based framework that:

1. captures progressive site layout changes across multiple construction phases,
2. integrates both relocation and installation costs to ensure economic feasibility,
3. employs a risk-based, multi-tiered prioritization system to focus coverage on critical zones,
4. supports adaptive strategies for maintaining, relocating, or deploying cameras in each phase, and
5. applies pre-processing techniques to reduce computational overhead while maintaining model linearity and solvability.

This formulation provides a robust yet practical solution for dynamic surveillance planning in construction environments, offering globally optimal outcomes that address both technical and economic dimensions.

The subsequent sections of the paper are organized as follows: Section 2 summarizes existing studies on the applications of surveillance cameras on construction sites and the optimal placement of cameras. Section 3 provides a detailed description of the proposed method. Section 4 examines the proposed method using field data from a construction site. The results are presented in Section 5. Section 6 discusses the findings and their implications. Finally, Section 7 concludes the paper by summarizing the main achievements.

2. Literature review

The use of networked camera surveillance systems has enabled real-time tracking of personnel, machinery, and construction activities through continuous and remote monitoring [14,18]. These systems generate visual data feeds that capture the spatial and temporal dynamics of construction entities, supporting various tasks such as safety monitoring, productivity assessment, and progress tracking. However, the success of these applications heavily depends on the strategic placement of surveillance cameras—including the type, number, and location—in response to evolving site conditions [14,18].

Prior studies on surveillance in construction environments generally fall into two conceptual categories: (1) Applications of Surveillance Cameras on Construction Sites and (2) Optimization of the Surveillance Camera Placement Problem (*SCPP*).

2.1. Applications of surveillance cameras on construction sites

Surveillance cameras are widely employed as data acquisition tools for a range of computer vision tasks, including object detection, tracking, activity recognition, and classification [19]. These capabilities have been utilized in numerous studies to automate essential functions such as hazard identification, resource and worker tracking, construction progress monitoring, and quality assessment.

Table 1 organizes the related literature based on the specific application domains within construction surveillance, highlighting the prevalence of object detection across all categories. Prior studies, as summarized in Table 1, can be categorized into four application domains: safety, productivity, progress monitoring, and quality control. Object detection remains the most frequently applied computer vision technique across these domains. While other methods, such as object tracking, activity recognition, and action or object classification, have also been used, particularly in safety and productivity applications, object detection is predominantly employed in quality control tasks.

While advancements in computer vision have enhanced data interpretation capabilities, the placement strategy of surveillance cameras—a critical determinant of data quality—has received far less attention. Improperly positioned cameras can lead to occluded views, blind spots, and degraded visual input, ultimately undermining the effectiveness of subsequent computer vision analysis.

To fill this gap, the present study introduces an optimized camera placement framework aimed at maximizing data utility. The model dynamically allocates camera positions to minimize occlusions and ensure comprehensive monitoring of high-risk and high-priority areas. This targeted placement strategy significantly improves the performance of automated surveillance in key application areas:

- *Safety Monitoring*: By maintaining unobstructed views of hazardous zones, the system enables early detection and real-time intervention.
- *Productivity Assessment*: Improved tracking of workers and machinery facilitates more precise evaluation of performance metrics.
- *Progress Monitoring*: Enhanced coverage supports the reliable collection of visual data, assisting in the automated tracking of construction progress and the early identification of potential delays.
- *Quality Control*: High-resolution visual data enable accurate detection of material defects and construction anomalies.

Through these improvements, the proposed model considerably enhances the input quality required for computer vision tasks. Additionally, by eliminating redundant or inefficiently placed cameras, it reduces data processing overhead, thereby improving the overall efficiency of computer vision systems.

2.2. Surveillance camera placement problem (SCPP)

The foundational research on *SCPP* is often attributed to the Art

Table 1
Related work on the application of surveillance cameras.

Reference	Safety				Productivity				Progress Monitoring				Quality Control
	Object detection	Object tracking	Activity recognition	Classifying actions/objects	Object detection	Object tracking	Activity recognition	Classifying actions/objects	Object detection	Object tracking	Classifying actions/objects		Object detection
[20–28]	✓												
[8,29–32]			✓										
[33]			✓	✓									
[34–40]	✓	✓											
[41–44]	✓				✓								
[29,31,45–48]		✓	✓				✓						
[49]							✓	✓					
[50–55]							✓						
[10,11,38,56–60]					✓	✓							
[60]							✓	✓					
[40,61–64]									✓				
[65,66]									✓		✓		
[67]									✓	✓			
[12,28,68–76]													✓
Sum	20	13	10	1	12	8	8	2	8	1	2		11

Gallery Problem (*AGP*) [77], a computational geometry problem focused on optimizing visibility using the fewest number of guards. Both *SCPP* and *AGP* seek to maximize coverage with minimal resources [78–80]. In mathematical terms, the *AGP* involves a simple polygon P (without holes or self-intersections). A guard c $(c \in P)$ is considered to observe a specific region G where $G \in P$. A point q lies within the observation area of guard c if and only if the direct line between q and c is entirely contained within the polygon P $(\overline{qc} \subseteq P)$ [77] (Fig. 1).

Although *AGP* and *SCPP* share similarities—which could suggest that the Surveillance Camera Placement Problem (*SCPP*) is a generalized version of *AGP* —they have some key differences. The main distinction involves the Field of View (*FOV*) and the Angle of View (*AOV*). The *FOV*, which represents the total area a camera can monitor, depends on the *AOV*, which defines the angle through which the camera captures its surroundings. A typical healthy human guard has an *AOV* of about 120° [81,82]. In contrast, within the context of *SCPP*, the *AOV* can vary significantly, ranging from 30° to 180°, depending on the lens type and sensor size.

Another significant difference between *AGP* and *SCPP* lies in the dynamic nature of the construction environment. In detail, construction sites are constantly changing as obstacles and walls are built and demolished, making it difficult to identify stable and secure locations for camera installation. Art galleries, on the other hand, have static layouts that allow for the permanent placement of surveillance equipment.

These unique characteristics introduce additional complexities into camera placement decisions on construction sites, particularly when planning must occur before construction begins to avoid costly modifications during implementation [18]. A considerable number of research efforts have addressed the problem of camera placement optimization, most of which focus on non-construction environments. Table 2 summarizes the most cited papers based on several key categories, including project type, surveillance objective (e.g., minimum cost, maximum or specified coverage, or 100 % coverage), workspace dimensionality (2D or 3D), site layout condition (static, phase-based dynamics, or dynamic model), mathematical model type (ILP, INLP, MILP, or MINLP), and the nature of the solution method employed (exact or approximate).

As can be seen from Table 2, the following results can be obtained:

- Most of the methods introduced in recent years have used field data obtained from surveillance cameras for validation.
- Most research focuses on optimizing coverage while minimizing costs; few attempts have been made to achieve 100 % coverage due to practical and financial constraints.
- The Integer Linear Programming (*ILP*) method is the most commonly used in this field, aiming to determine optimal surveillance camera locations.

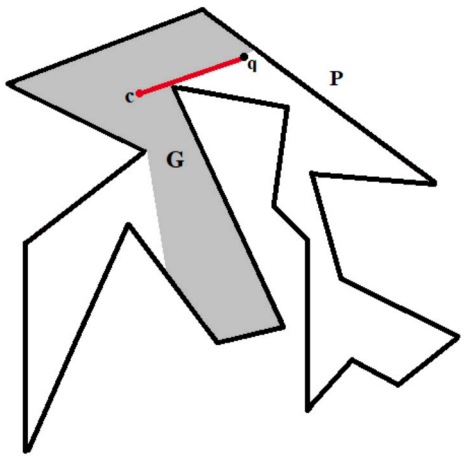

Fig. 1. Visualization example of *AGP*.

Table 2
Comparing prior research to current study.

Reference	Project Type	Objective(s)			Workspace		Site Layout			Mathematical Model				Solution Method	
		Minimum Cost	Maximum/ Specified Coverage	100 % Coverage	2D	3D	Static	Phase-Based Dynamics	Dynamics Model	ILP	INLP	MILP	MINLP	Exact	Approximate
[83]	University Campus		✓		✓		✓			✓				✓	
[14]	Construction site	✓	✓		✓		✓				✓				✓
[18]	Metro Station			✓		✓		✓		✓					✓
[84]	Large-scale project	✓	✓		✓		✓						✓		✓
[85]	Building (Indoor)	✓	✓			✓	✓					✓			✓
[9]	Construction site	✓	✓			✓		✓			✓				✓
[86]	Building (indoor)		✓		✓			✓			✓				✓
[87]	City level	✓	✓			✓	✓			✓					✓
[88]	Bridge	✓	✓			✓	✓			✓					✓
[89]	Island	✓	✓			✓	✓				✓				✓
[90]	Building (Indoor)	✓	✓			✓	✓			✓					✓
[91]	University Campus	✓	✓		✓		✓			✓					✓
This paper	Construction site	✓	✓		✓				✓			✓		✓	

- Few studies have focused on finding exact (globally optimal) solutions that guarantee the best possible solution for camera placement.
- The majority of methods introduced for construction applications assume a static surveillance environment, meaning the positions of targets and obstacles remain constant over time. Only a few studies have considered construction dynamics; none have accounted for relocation costs or incorporated dynamic changes within their mathematical models. *Re*-optimization using mathematical formulations has been limited to a small number of discrete layout plans.

In contrast to prior studies, this research introduces a risk-aware and dynamically adaptive optimization model for surveillance camera placement in construction environments. The model is formulated as a Mixed-Integer Linear Program (*MILP*) and solved using exact algorithms to ensure global optimality— overcoming the limitations of most existing methods that rely on heuristic or metaheuristic solvers. A key advancement lies in the model's explicit incorporation of site evolution across all construction phases, allowing it to capture continuous physical changes in layout and risk zones. At each phase transition, the model intelligently decides whether to add new cameras or reconfigure existing ones to maintain the coverage level required by the project manager while minimizing equipment costs. This adaptive decision-making process is fully embedded within the mathematical formulation, which accounts for both camera relocation and purchasing expenses, thereby addressing real-world budgetary constraints.

Additionally, the model significantly enhances surveillance efficiency by implementing a four-tiered risk-based prioritization scheme. This structure ensures that critical zones are continuously monitored while deliberately excluding low-risk or completed areas from unnecessary surveillance, thereby avoiding cost-intensive over-coverage—an issue frequently neglected in previous research. By dynamically aligning camera layouts with evolving risk profiles and spatial configurations, the model delivers a cost-effective and operationally viable surveillance strategy.

3. Methodology

The proposed method is structured into a modular three-layer architecture, as illustrated in Fig. 2, to support the optimization of surveillance camera placement on dynamic construction sites:

- **Input Layer:** This layer gathers all necessary raw data and project-specific information, including the site floor plans for each phase, known physical obstacles, candidate camera installation locations, and user-defined monitoring objectives.
- **Processing Layer:** This layer is responsible for transforming the input into a mathematically tractable format for optimization. First, the environment is discretized through meshing. Next, surveillance priority is assigned to each cell based on predefined risk levels. In this study, four priority classes are used—Priority 1 (Red), Priority 2 (Orange), Priority 3 (Yellow), and Priority 4 (White, indicating non-critical areas). Finally, the MILP-based optimization is implemented, integrating camera specifications, relocation costs, and temporal dynamics across phases.
- **Output Layer:** The final layer generates practical and applicable outputs that support both strategic planning and on-site implementation. As shown in Fig. 2, this includes the optimal camera layout for each construction phase, clearly reflecting the dynamic nature of the project and how the system adapts camera positions over time. Additionally, a cost-coverage trade-off analysis is provided to inform decision-makers of the financial implications of different coverage levels and camera types. It also highlights the model's extensibility and real-world adaptability.

In the next section, each step is elaborated in detail.

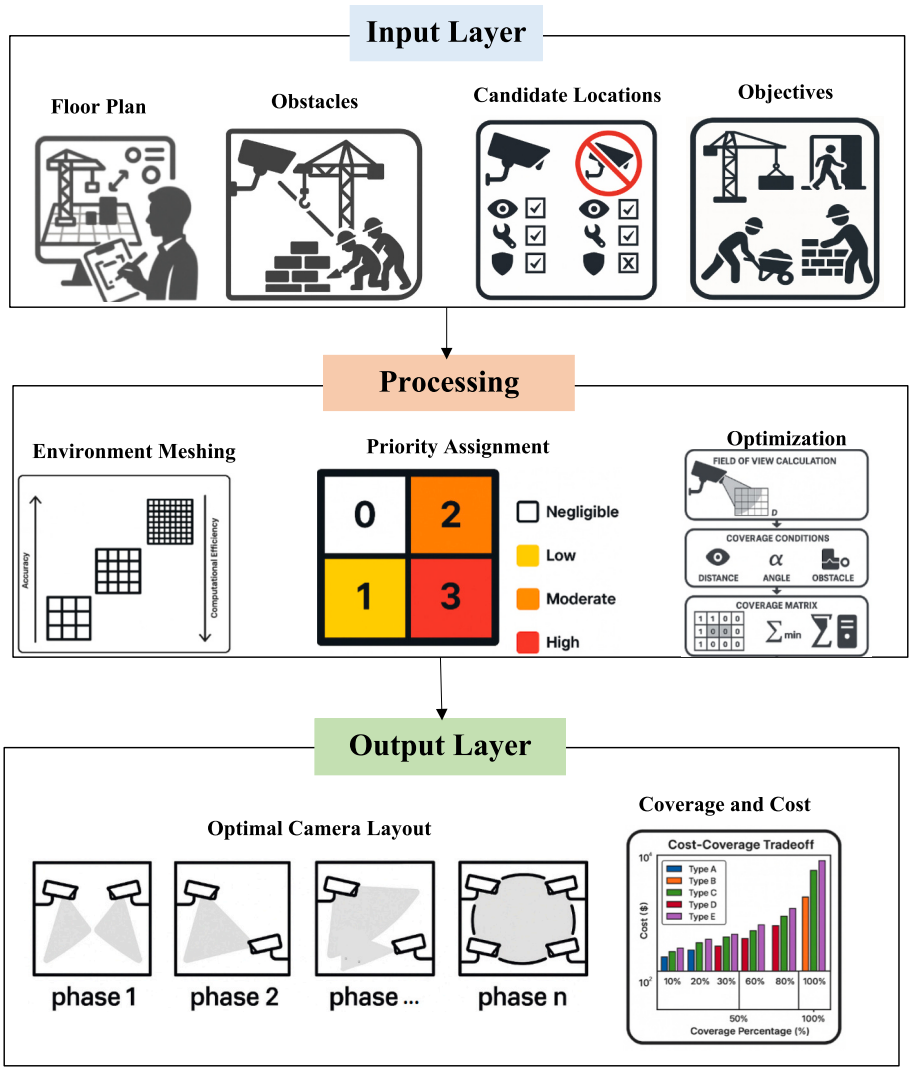

Fig. 2. Proposed camera placement optimization framework.

3.1. *Environment modeling*

The environment modeling step is essential for establishing a foundation for camera placement optimization. It translates the physical construction site layout into a digital representation that can be effectively analyzed and interpreted by the model. In this section, we clarify the process of modeling the construction project environment for the Surveillance Camera Placement Problem (*SCPP*).

- **Process**

The modeling process comprises three key stages:

1. **Creating Digital Site Model:** We convert the *CAD* drawing of the construction site layout into a high-resolution digital image. This image serves as the basis for modeling and analysis. The project manager annotates this image to denote the location and dimensions of equipment and materials, ensuring an accurate representation of spatial constraints and active areas.
2. **Obstacle Identification:** Obstructions are defined as any features or structures that hinder visibility, such as walls, storage units, vehicles, or temporary construction equipment. The identification of obstructions involves analyzing the annotated image to specify elements that block the direct line of sight between potential camera placements and their target areas. This is achieved through visual inspection and spatial analysis techniques that assess the proximity of objects within the model.
3. **Candidate Location and Target Area Identification:** Potential camera locations are identified based on three criteria:

- *Visibility*: Candidate locations must provide unobstructed views of designated target areas.
- *Accessibility*: Selected locations should facilitate easy installation, maintenance, and potential relocation of cameras.
- *Structural Integrity*: Chosen positions must be structurally sound and capable of supporting the cameras.

Suitable locations for cameras may include permanent structures (e.g., walls, columns), semi-permanent installations (e.g., cranes, scaffolding), and boundary assets (e.g., fences). Target monitoring areas are defined based on the project phase and risk assessment, prioritizing regions such as entry/exit points, high-risk zones, material storage areas, and high-traffic worker zones.

- **Model Inputs and Outputs**

The inputs include a digital image generated from the construction site layout CAD drawing, alongside engineer-provided annotations that specify the location and dimensions of equipment and materials.

The corresponding output is a digital representation of the site that highlights obstructed areas, candidate camera installation positions, and designated surveillance targets.

To ensure adaptability to construction site dynamics, updates are conducted at major phase transitions. These updates incorporate changes in site layout, risk-priority zones, and visibility obstructions, which are manually integrated into the optimization model. The proposed process follows an adaptive methodology to facilitate updates, making it reusable across different projects. While currently manual, future research could automate this process using *BIM* integration, *IoT*-enabled sensors, and *AI*-driven risk assessment to support real-time surveillance optimization.

3.2. Environment meshing

To represent a target location as a set of distinct cells, meshing is a commonly used method in mathematical modeling [86,92]. The size of the cells is an important factor to consider during the process of discretizing the desired location [93]. While smaller unit cells can increase precision, they may also reduce computational efficiency.

To perform this step, we convert the *CAD* drawing of the construction site layout into a high-resolution digital image that serves as the input. This image is then divided into discrete unit cells through a meshing process. Information such as whether individual cells represent obstacles or work areas, their relative grid positions, and their assigned surveillance priorities can be retrieved for each cell. The size of each cell used in this study was set to 1×1 m^2.

3.3. Determining surveillance priority

After environmental modeling and meshing, establishing the priority of each cell is essential to ensure efficient surveillance planning. As previously mentioned, assigning equal importance to all areas of a construction site is neither practical nor economical. To address this, the proposed model adopts a risk-based prioritization strategy, assigning weights to cells based on their relative importance in terms of safety, asset protection, and operational criticality (See Table 3)

In this study, the surveillance area is categorized into four levels of priority (0–3), following consultations with experienced site engineers and safety managers. This classification is based on factors such as historical incident data, frequency of worker activity, and the presence of high-risk equipment or operations. The four-level system is as follows:

- Level 3 (High Priority): Zones with intense, high-risk activities such as crane operations, excavation pits, and structural assembly work.
- Level 2 (Moderate Priority): Areas used for material staging or equipment storage, which may pose theft and fire risks.
- Level 1 (Low Priority): General access pathways and temporary workspaces with lower activity.
- Level 0 (Negligible Priority): Perimeter or completed areas where no active construction work is taking place.

This structured classification aligns with the *PMBOK* (Project Management Body of Knowledge) guidelines (Sections 11.2 and 11.3), which emphasize systematic risk identification and qualitative analysis. Moreover, by minimizing unnecessary monitoring in non-critical zones, this approach improves cost-efficiency while maintaining robust surveillance in high-risk areas.

The assigned weights (*Wtj*) are dynamically updated throughout the project based on changes in layout and risk level. These updates are manually integrated in the current implementation but could be automated in future studies using technologies such as *BIM*, *IoT*-based sensors, or *AI*-driven risk detection. The flexible structure of the model supports both manual and automated workflows, allowing practitioners to tailor data acquisition frequency and methods based on project needs and available resources.

Table 3
Weighting of coverage candidate areas.

Cell coverage weight (W_{tj})	Color	Risk level
0	White	Safe
1	Yellow	Low risk
2	Orange	Medium risk
3	Red	Dangerous

Ultimately, the surveillance priority map is incorporated into the optimization workflow to reflect current site conditions. This enables the system to adapt to evolving risks and maintain effective coverage without incurring unnecessary costs.

3.4. Camera coverage

In this research, camera coverage is defined by two primary parameters: Angle of View (*AOV*) and visible distance. These parameters are directly derived from the specifications of the cameras used, and they play a crucial role in determining the effectiveness of surveillance on dynamic construction sites.

(i) Angle of View (*AOV*)

The *AOV* defines the angular extent of the camera's Field of View (*FOV*), influencing the width of the area covered by the camera. Cameras with a wider *AOV* can monitor larger areas but may capture fewer details, whereas a narrower *AOV* provides more detailed coverage of a smaller area (Fig. 3). The *AOV* is particularly important in optimizing camera placement, as it determines the spatial layout of camera coverage zones.

(ii) Visible Distance.

The visible distance, determined by the surveillance camera's inherent technical specifications (e.g., focal length, image resolution, sensor size), is not a configurable modeling parameter but rather a fixed characteristic of each camera model. However, simply capturing an image at the maximum range does not guarantee its usefulness for surveillance purposes. The effective monitoring range—the distance at which the image quality is sufficient for meaningful observation—depends on the required level of detail.

To address this, we adopt the internationally recognized performance guidelines defined by the International Electrotechnical Commission (*IEC*), particularly the *IEC 62676–4:2015* standard [94]. This

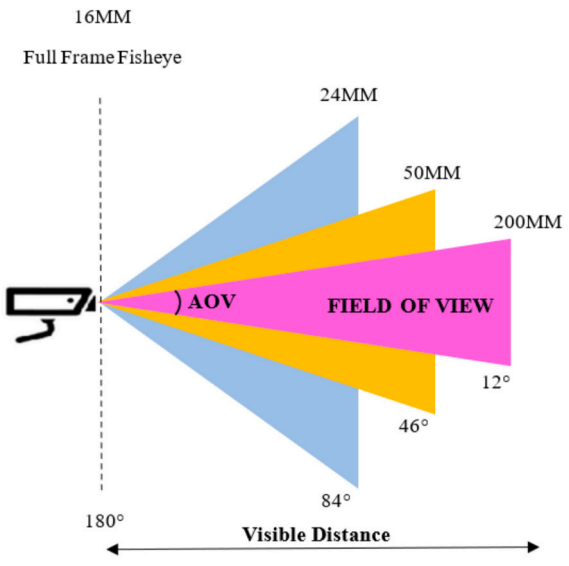

Fig. 3. Camera coverage modeling examples.

standard establishes pixel density thresholds for different levels of surveillance functionality:

1. *Detection*: Objects are observable but lack detailed characterization. For instance, a moving vehicle may be detected without identifying its type (See Fig. 4.).
2. *Recognition*: Elementary characteristics of objects become distinguishable. For example, a detected vehicle can be identified as a truck (See Fig. 4.).
3. *Identification*: Detailed recognition is possible, such as identifying a specific person or distinguishing between similar objects (See Fig. 4.).

In this study, the Detection level is selected as the baseline for calculating camera coverage. This decision was made in consultation with the project manager and reflects a practical trade-off between monitoring needs and resource limitations. On construction sites, situational awareness is typically more important than high-resolution identification. The detection-level threshold provides sufficient functional coverage while maintaining manageable installation costs and computational efficiency.

It is important to emphasize that the optimization model is designed to be flexible and configurable. While the detection level has been determined based on the specific monitoring objectives and resource limitations of the current project, researchers can adjust the effective visual range to suit the particular needs of their respective projects and the operational conditions of their construction sites.

3.5. Mathematical modeling

To set up surveillance cameras effectively in a given area, it is necessary to understand how to maximize their Field of View (*FOV*) within the spatial constraints of the site. This study introduces a mathematical model designed to minimize the costs associated with deploying surveillance systems in dynamic construction environments, addressing both fixed and variable factors that influence the optimal number and placement of cameras. By incorporating these dynamic and cost-related factors into the optimization process, we ensure that the proposed approach is not only efficient but also adaptable to the evolving needs of a construction site.

Mixed-Integer Linear Programming (*MILP*) problems can be addressed using either exact or heuristic algorithms. In this study, an exact algorithm was selected to solve the *MILP* formulation to improve both cost-efficiency and operational performance. Achieving a globally optimal solution considerably improves both cost-efficiency and operational performance by reducing redundant expenditures and removing suboptimal camera placements—an essential consideration in budget-constrained applications such as construction site surveillance.

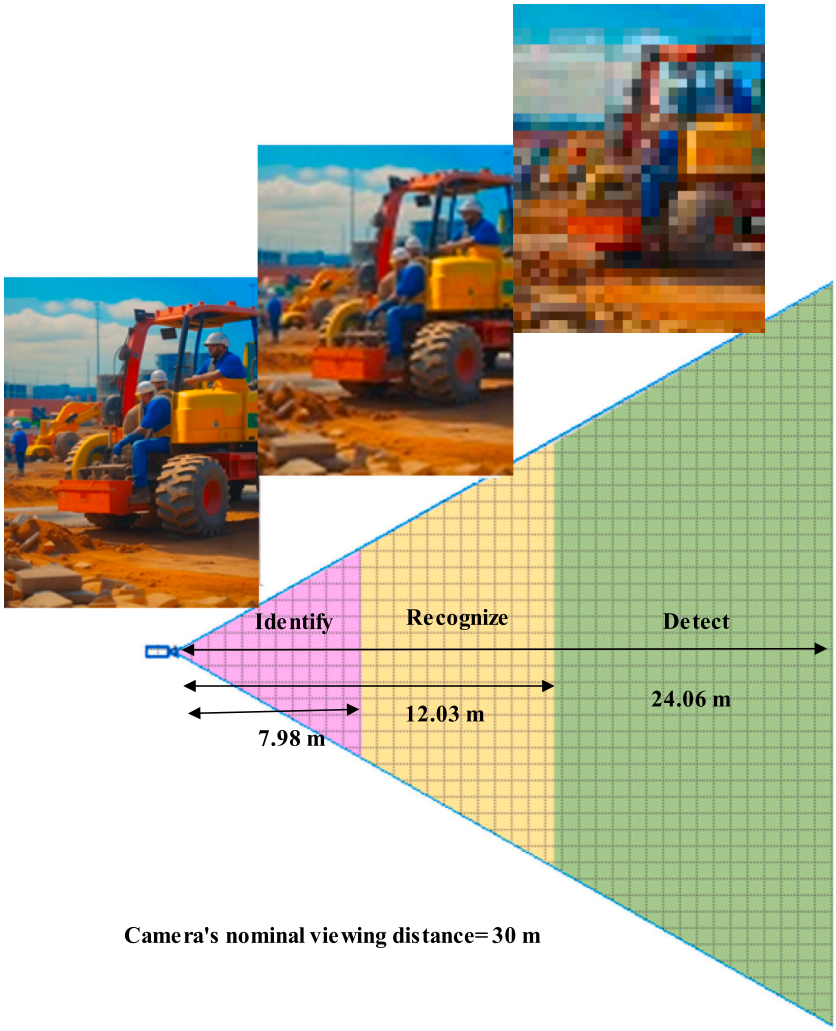

Fig. 4. FOV (Field of View) components in the camera.

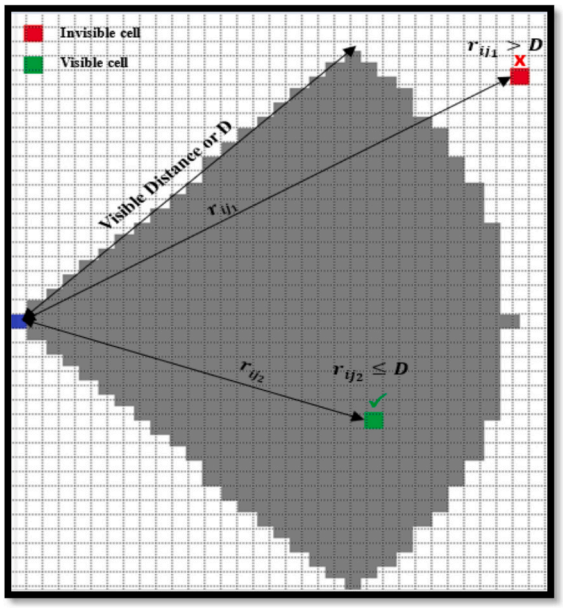

Fig. 5. Coverage criteria: condition 1

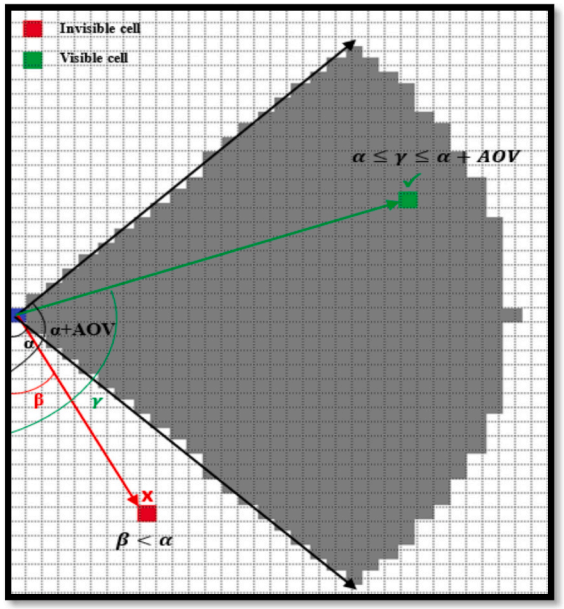

Fig. 6. Coverage criteria: condition 2

The proposed approach ensures a globally optimal solution (within the problem scale and available computational resources), which is an important consideration in construction site surveillance where suboptimal camera placements may lead to inadequate coverage and increased safety risks. While heuristic and metaheuristic approaches offer improved computational efficiency, they do not provide the same guarantees of optimality. To further enhance the practical solvability of the problem and facilitate the exact solution, some decision variables were transformed into parameters prior to the optimization process. This modeling choice reduced the computational burden, contributing to the feasibility of obtaining an exact solution within the available computational resources.

To implement this, we first present an innovative step-by-step approach for calculating the *FOV* for each camera based on its mounting position and any visual obstructions. Fig. 5 illustrates a scenario in which a camera is positioned at location i, where $i \in I$ and I is the set of candidate locations. The gray cells represent the coverage area of this camera, determined by its Angle of View (*AOV*) and coverage radius D. The visible area (μ_{ij}) is depicted by these gray cells.

A cell j ($j \in J$) falls within the visible range of a camera located at i if the following three conditions are met:

1. **Distance Condition**: The distance between the target cell j and the camera at location i must not exceed the coverage radius of the camera D (Eq. (1)).

$$r_{ij} \leq D \tag{1}$$

where r_{ij} denotes the distance between the camera located at cell i and the target cell j.

2. **Angle of View Condition**: The target cell j must be positioned within the Angle of View *(AOV)* of the camera located at position i (Eq. (2), Fig. 6).

$$\alpha \leq \gamma \leq \alpha + \mathrm{AOV} \tag{2}$$

3. **Obstacle Condition**: Eq. (3) is used to ensure that no obstacle exists between the camera at location i and the target cell j. Fig. 7 illustrates this condition by showing a straight line between i and j. Eq. (3) constrains the coverage area defined by Eq. (1) and Eq. (2).

$$y_{obs} - y_i \neq \left(\frac{y_i - y_j}{x_i - x_j}\right)(x_{obs} - x_i) \forall (x_{obs}, y_{obs}) \in P \tag{3}$$

where:

(x_i, y_i): the coordinates of the camera located at position i.

(x_j, y_j): the coordinates of the target cell j

(x_{obs}, y_{obs}): the coordinates of a view-obstructing cell

Set P contains all the view-obstructing cells.

Failure to meet any of the aforementioned conditions will result in classifying the target cell j as *uncovered* by the camera located at i. The

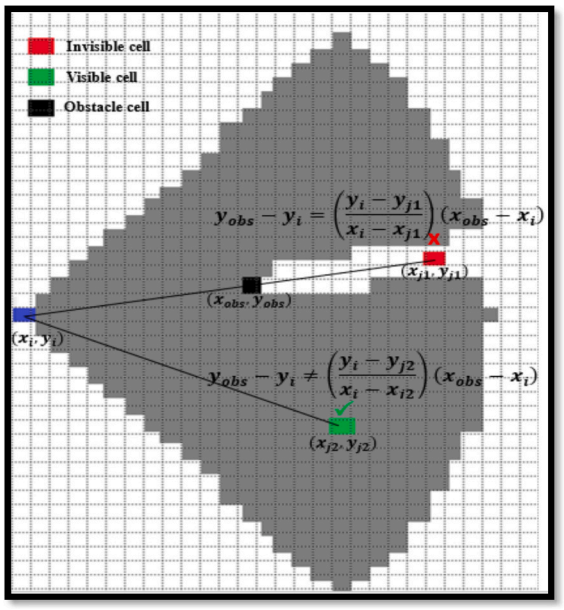

Fig. 7. Coverage criteria: condition 3.

calculated coverage area for each camera is stored in matrix C_i, where covered cells are represented by a value of 1 and uncovered cells by a 0.

After obtaining the coverage matrix for each candidate location, a Mixed Integer Linear Programming (*MILP*) model is developed to minimize surveillance costs while ensuring that the desired coverage rate is met. The objective function and constraints of the model are detailed as follows:

$$Z = \min \left[C \times NC + \sum_i x_{i1} \times f_i + \sum_i \sum_{t=2}^{NT} y_{it} \times f_i + \sum_i \sum_{t=2}^{NT} \bar{y}_{it} \times \bar{f}_i + \sum_i x_{iNT} \times \bar{f}_i \right] \quad (4)$$

$$y_{it} \geq x_{it} - x_{i(t-1)} \ \forall_{i,t=2,\ldots NT} \quad (5)$$

$$\bar{y}_{it} \geq x_{i(t-1)} - x_{it} \ \forall_{i,t=2,\ldots NT} \quad (6)$$

$$\frac{\sum_j z_{tj} \times w_{tj}}{\sum_j w_{tj}} \geq CR_t \ \forall_t \quad (7)$$

$$x_{it} \times \mu_{itj} \leq z_{tj} \ \forall_{i,t,j} \quad (8)$$

$$\sum_i x_{it} \times \mu_{itj} \geq z_{tj} \ \forall_{t,j} \quad (9)$$

$$x_{it} \leq \sum_j \mu_{itj} \ \forall_{i,t} \quad (10)$$

$$NC \geq \sum_i x_{it} \ \forall_t \quad (11)$$

To clarify the model formulation, Table 4 provides definitions of the variables and parameters used.

The objective function of the proposed model (Eq. (4)) is formulated to minimize the overall cost associated with the dynamic deployment strategy of cameras. This formulation considers various factors, such as the relocation and removal of cameras during different project phases, while ensuring that the required coverage is maintained through constraints governing camera movement and redundant coverage calculations. The objective function comprises five distinct cost components, each representing a different aspect of the camera placement process. These components are detailed as follows:

1. **Purchase**: The first term accounts for the total expenditure on acquiring the required number of cameras.
2. **Initial Installation**: The second term captures the total cost of installing all cameras during the initial phase of the project.
3. **Movement**: The third term represents the total cost of moving cameras across different phases of the project.
4. **Intermediate Removal**: The fourth term covers the total cost of removing cameras during intermediate phases of the project.
5. **Final Removal**: The final term accounts for the total cost of removing all cameras at the end of the project.

It is important to note that the parameters of the model were derived using both theoretical and empirical approaches. Specifically, for determining the cost parameters f_i and $\bar{f}_i$, we employed an empirical approach. While this method was used, alternative approaches can also be considered to define these parameters. For instance, theoretical frameworks such as multi-criteria decision-making techniques can be utilized to systematically derive parameters based on established criteria and priorities. Users could define parameter values using methodologies that align most effectively with the unique requirements and constraints of their specific project.

Constraint (5) ensures that a camera can only be relocated to a new position if it was previously installed at another location. Constraint (6) ensures that a camera can only be removed if it was previously installed. Constraint (7) guarantees that the required coverage, as defined by the project manager, is met or exceeded at all phases of the project lifecycle.

A notable innovation in the proposed model is the introduction of the decision variable z_{tj}, which plays a key role in enhancing computational efficiency by reducing redundant coverage calculations. Typically, models may recompute coverage for a given zone multiple times if it falls within the field of view (*FOV*) of several cameras. The variable z_{tj} in Eq. (7) directly addresses this inefficiency. Eqs. (8) and (9) define the permissible range of values for z_{tj} and determine its relationship with the decision variable x_{it} and the coverage parameter μ_{itj}. Specifically, z_{tj} is assigned a value of 1 if, and only if, cell j is monitored by at least one camera, regardless of the number of cameras covering that cell. Eq. (9) ensures that if cell j is covered in phase t (z_{tj}=1), then at least one camera located at i must be installed and covering that location. Eq. (10) ensures that each camera is assigned to cover at least one cell. The number of cameras installed in each phase does not exceed the minimum number of cameras required (Eq. (11)).

The proposed approach utilizes *Python* 3.12.1 [95] (VS *Code* editor 1.89.1 [96]) to transform site layout maps related to various project phases into numerical data and employs the *IBM CPLEX Optimization Studio* [97] to solve the proposed Mixed-Integer Linear Programming (*MILP*) model. *CPLEX* is a widely recognized optimization tool that uses classical algorithms, such as branch-and-bound, to solve complex problems efficiently. While CPLEX served as the solver for this research, it is important to note that the development or improvement of the branch-and-bound algorithm itself was not the focus of this work. The extensive validation of *CPLEX* across countless research studies highlights its practical effectiveness, making it an appropriate choice for the objectives of this study. Finally, the optimization results are depicted using *Python*. To provide an opportunity to replicate the proposed method and encourage further

Table 4
Nomenclature.

Symbol	Description	Type
i	Index of camera candidates	Parameter
j	Index of target areas	Parameter
t	Index of time periods	Parameter
NT	Number of project phases	Parameter
C	Purchase cost of each camera	Parameter
f_i	Camera installation cost at location i	Parameter
$\bar{f}_i$	Camera removal cost from location i	Parameter
CR_t	Coverage requested of project manager in phase t	Parameter
w_{tj}	Coverage weight of cell j in phase t	Parameter
μ_{itj}	Parameter indicating whether a camera placed at location i in phase t covers cell j	Parameter (binary)
NC	Number of cameras	Decision Variable
x_{it}	Variable indicating whether a camera is installed at location i in phase t	Decision Variable (binary)
y_{it}	Variable indicating whether a camera is moved to location i in phase t from another location	Decision Variable (binary)
$\bar{y}_{it}$	Variable indicating whether a camera is removed from location i in phase t	Decision Variable (binary)
z_{tj}	Variable indicating whether cell j is monitored by at least one camera in phase t	Decision Variable (binary)

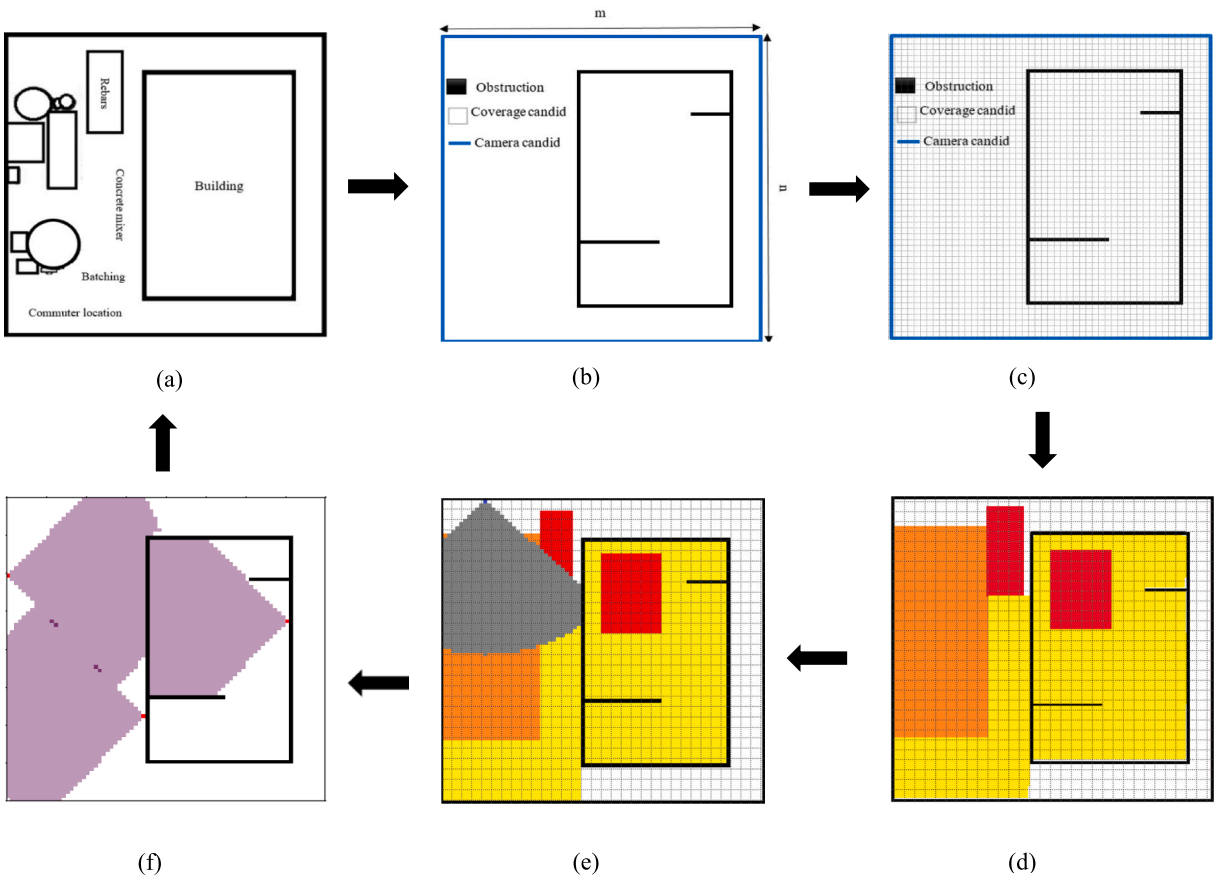

Fig. 8. Schematic representation of optimizing camera placement step: (a) Initial Layout Representation; (b) Defining Obstacles, Coverage Zones, and Camera Placement Candidates; (c) Grid-based Discretization of the Layout; (d) Risk Analysis; (e) Coverage Analysis; (f) Final Optimized Coverage Map.

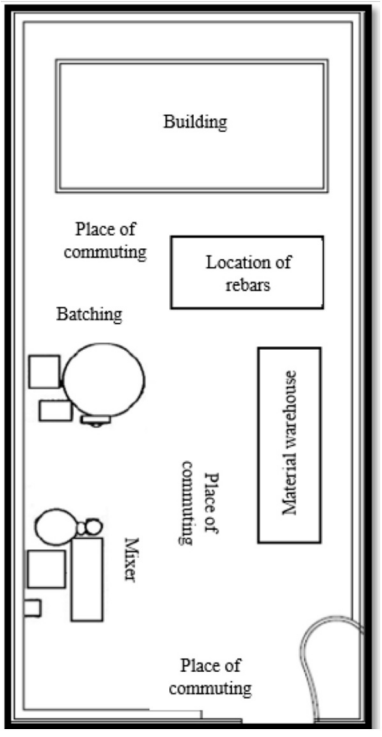

Fig. 9. Current design of the construction site.

Table 5
Specifications of case study.

Building dimensions	30 × 20 m
Project progress	Roughing
Dimensions of mesh networks	1 × 1 m
Number of meshes	3200

advancements in the field, we have made all the developed codes and case study data publicly available on the project's GitHub repository (*https://github.com/smartconstructiongroup/Camera_Placement_Optimization*).

The progressive stages of the proposed approach, up to achieving the globally optimal arrangement, are schematically depicted in Fig. 8. In Fig. 8, the blue areas indicate candidate locations for camera installation, the black areas represent obstacles to the camera view, and the white areas represent the target monitoring zones.

4. Case study

A case study of a residential construction project with an area of 3200 m^2 in Mashhad, Iran, was conducted to validate the proposed method. The site dimensions are 80 m by 40 m. Fig. 9 presents the current layout of the construction site, and Table 5 summarizes key project details.

During this project, the monitoring area changed significantly due to evolving site layouts. This research focused on optimizing *CCTV* camera placement during four key construction stages: foundation, frame and roof, roughing, and finishing. The proposed model adapted effectively to the changing layout in each phase, consistently ensuring the coverage levels required for designated priority areas—as defined by the project manager—to minimize unnecessary costs.

Table 6
Details on the types of cameras used.

Camera type	AOV (°)	Distance vision (m)				C ($)	f_i ($)	$\bar{f}_i$ ($)
		Written	Detect	Recognize	Identify			
A	120	80	28.22	14.11	9.36	142	15	10
B	47	50	48.64	24.32	16.13	281	15	10
C	87	80	38.93	19.46	12.91	187	15	10
D	113	60	29.97	14.98	9.94	175	15	10
E	92	50	24.85	12.42	8.24	90	15	10

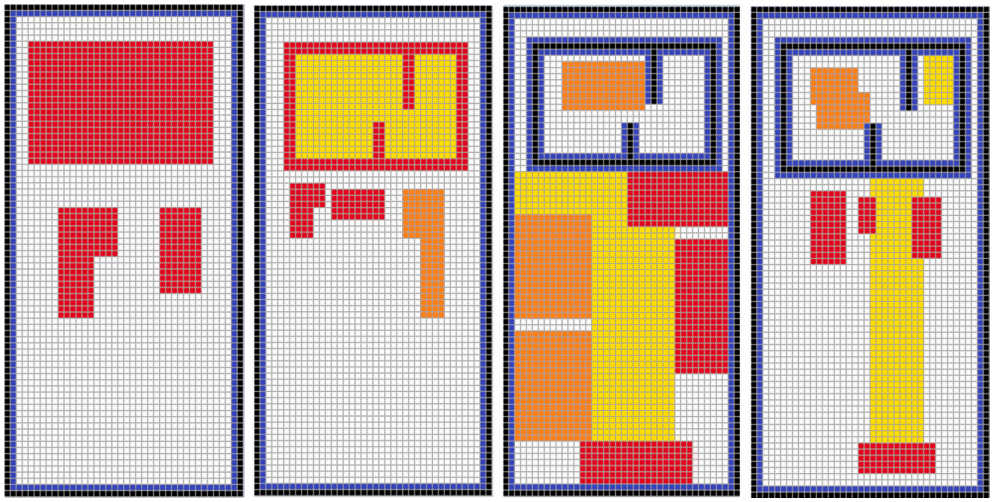

Fig. 10. Weighted site layout for various construction phases: (a) Foundation; (b) Frame and roof; (c) Roughing; (d) Finishing.

Furthermore, this study sought to optimize camera locations not only in outdoor areas but also within indoor spaces, such as inside buildings. The monitoring process aimed to determine the optimal camera type from among five available surveillance models, whose specifications are listed in Table 6. This case study was selected solely to demonstrate the proposed method; however, researchers can replicate the method with different case studies using the developed code available in the project's GitHub repository (*http://github.com/smartconstruction group/Camera_Placement_Optimization*).

5. Results

As construction progresses through its various phases, considerable changes occur in the site layout and the distribution of obstacles. These changes require ongoing monitoring and adjustments to camera locations to ensure that key areas are adequately covered while minimizing surveillance in unimportant zones. To address this challenge, the proposed model continuously adjusts camera placements to accommodate changes in site layout and environmental conditions.

The study presents a series of site layouts considered during the research, which are depicted in Fig. 10, along with an analysis of the differences between them and the corresponding need for adjustments at various stages of the construction process.

In the foundation phase (Fig. 10(a)), the site is largely free of obstructions, allowing perimeter-mounted cameras to record wide site views with minimal obstruction. As the project moves into the framing and roofing phase (Fig. 10(b)), the construction of vertical structures—such as pillars, walls, and the roof framework—brings about notable changes to the site layout. Consequently, it may become necessary to adjust the positioning of existing cameras or add new ones to maintain the required coverage.

In the roughing phase (Fig. 10(c)), additional support elements, windows, and framing considerably increase the complexity of the environment. Constructions, equipment, and materials generate more occlusions, reducing the coverage of existing cameras. As the project enters the finishing phase (Fig. 10(d)), interior walls, floors, and ceilings are introduced, thereby altering the space plan. New blind spots are introduced that may need additional cameras placed in the newly formed interior spaces and corridors. Key areas like exit doors, entryways, and construction zones where activities or materials are concentrated become critical areas for surveillance, and the location of cameras in relation to these spaces should be given sufficient attention.

Finally, the dynamic nature of construction sites necessitates a flexible and responsive approach to surveillance camera placement. Our study demonstrated the necessity of continuously relocating camera positions to accommodate the dynamic layout and environmental changes at each construction stage. This dynamic adjustment can be effectively realized through the implementation of our newly proposed model via camera relocation. The results are not limited to on-site security and enhanced safety but also lead to optimized resource allocation, enabling the approach to be adapted to various construction scenarios and applied in real-time situations. To demonstrate the effectiveness of the approach, a case study is included that evaluates different camera types and coverage scenarios.

Five types of cameras (A, B, C, D, and E) with varying Angles of View (*AOV*), visible distances, and purchase costs (as detailed in Table 6) were evaluated. The SCPP was optimally solved for a case study to determine the lowest investment cost across ten scenarios with coverage rates ranging from 10 % to 100 %.

As anticipated, the overall cost of surveillance—including the purchase of cameras, along with the expenses related to installation, removal, and relocation throughout different phases of the project—rises in direct proportion to the desired coverage rate for each type of camera. Fig. 11 illustrates the optimization results, with each column representing the cost needed to achieve the respective coverage across the entire project. For instance, the orange column at 90 % coverage shows that the total cost of type B surveillance cameras, from initial installation to final removal, amounts to $1580 to reach 90 % coverage.

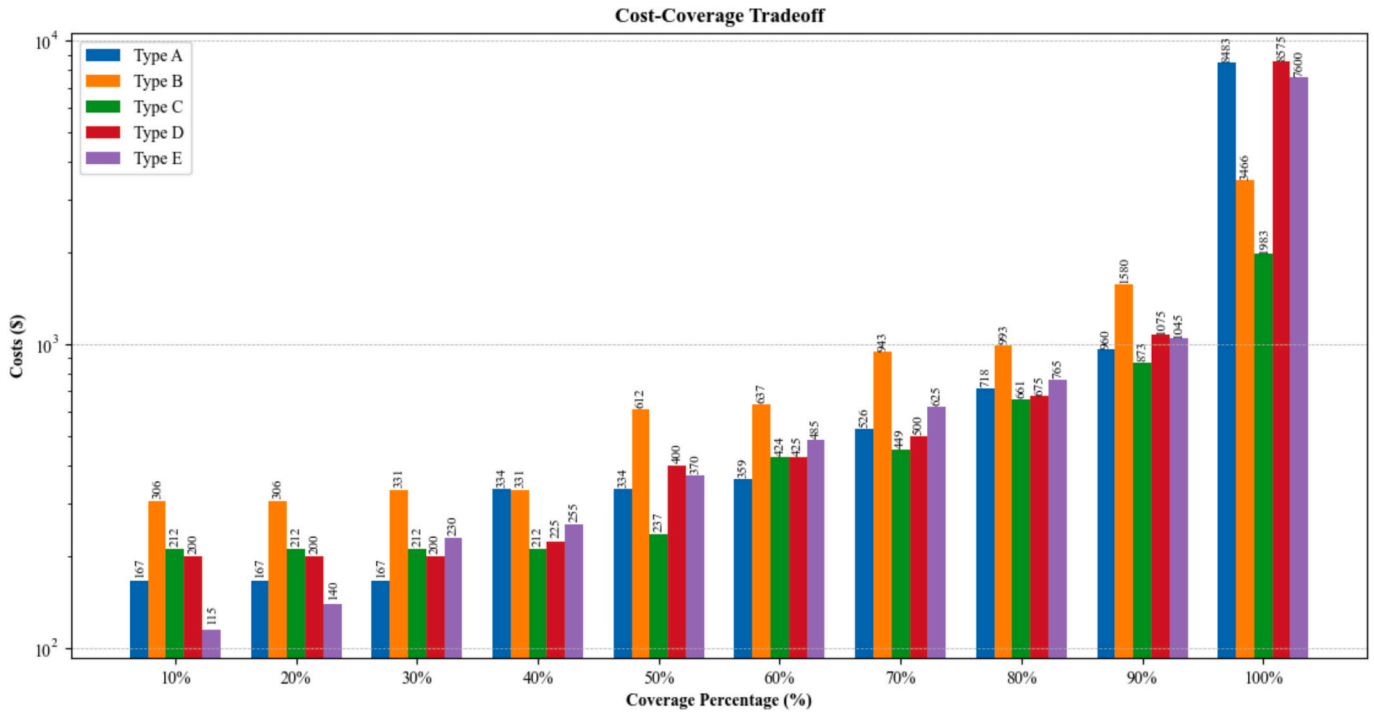

Fig. 11. Cost-Coverage tradeoff of different types of cameras.

As demonstrated, the selection of an optimal camera type notably impacts the overall monitoring costs. In fact, the type of camera that is most cost-effective will depend on the desired percentage of coverage. For instance, with a low coverage percentage, like 10 % to 20 %, the most cost-effective camera type is E with an overall monitoring cost of $115 and $140, respectively. On the other hand, the type C cameras are most appropriate for maximum coverage conditions (70 %–100 %). The related costs of type C vary from $449 to $1983. In contrast to these, the type A cameras are used in intermediate coverage conditions of 30 % and 60 %. The price for these ranges from $167 to $359.

By comparing the costs associated with different camera types across various coverage levels, project managers can make informed decisions to achieve the desired coverage while minimizing overall investment. Emphasizing the installation of cost-effective type E cameras in areas with low coverage needs, and expensive type C cameras in high-demand zones, helps to optimize the resources allocated for the project's surveillance requirements. The proposed procedure is cost-effective and provides efficient site monitoring throughout the construction process.

Moreover, this approach has the ability to create a layout within the limits of a maximum cost limit established by project managers. For instance, if the budget for surveillance cameras is restricted to $800 the most economical option as depicted in Fig. 11 is to position two type C cameras offering 80 % coverage at an expense of $661. This feature allows decision makers to customize a surveillance system that adheres to budgetary constraints while still meeting the desired coverage level.

Schematic representations of the optimal layouts for the scenarios examined during the roughing phase are illustrated in Fig. 12.

The optimal layouts shown in Fig. 12 for the scenario with full coverage depict four different shades of purple, each representing a specific level of coverage as detailed below:

- The lightest purple shade (A) signifies coverage by a single camera.
- The medium purple shade (B) signifies coverage by two cameras.
- The darker purple shade (C) signifies coverage by three cameras.
- The darkest purple shade (D) signifies coverage by four cameras.

The fact that there are no more than four overlaps in the complete coverage of the area being monitored highlights the efficiency and effectiveness of the proposed model. In particular, the model strategically places the cameras at distances to minimize overlap, reducing the total number of cameras needed while still achieving the required coverage.

In cases where indoor and outdoor areas are assigned equal priority weights, the model may naturally cover outdoor areas first. This is because outdoor locations often provide broader coverage due to fewer obstructions, making it more cost-effective. However, if a distinction between indoor and outdoor coverage is necessary, the model can be adjusted by assigning higher weights to indoor areas or applying specific constraints to prioritize indoor camera placement. This ensures that indoor spaces are covered earlier in the optimization process. This flexibility highlights the model's ability to address complex and specific requirements, as it is designed to be easily adaptable to different scenarios.

As previously discussed, achieving 100 % coverage of the environment is essentially impractical. The present study provides evidence to support this claim. The relationship between cost and coverage percentage is nonlinear, as illustrated in Fig. 11. At lower coverage percentages, the cost increases gradually. However, as coverage approaches 100 %, the increase in cost becomes significantly more pronounced. The use of a logarithmic scale on the y-axis effectively emphasizes the exponential cost escalation as coverage nears full completion. Specifically, for a 10 % increase in coverage from 90 % to 100 %, the total cost increases approximately eightfold for Type A cameras, twofold for Types B and C cameras, and sevenfold for Types D and E cameras. This substantial cost increase may not be economically viable, rendering it unfeasible for the current project.

While 100 % coverage of the surveillance site is theoretically desirable, it is usually impractical in real-world scenarios. Obviously, full coverage requires that every point in the area be covered; however, it often cannot be achieved because of limitations in places for camera installation. Fig. 11, for example, illustrates how 100 % coverage from type D cameras requires the excessive investment of $8575 and 41 cameras. It is possible to further reduce the monitoring cost to $2175 by setting up only four central cameras with a total sum of 10 cameras through various project phases, and achieving full coverage (See Fig. 13.). In practice, however, less than full coverage is usually achieved

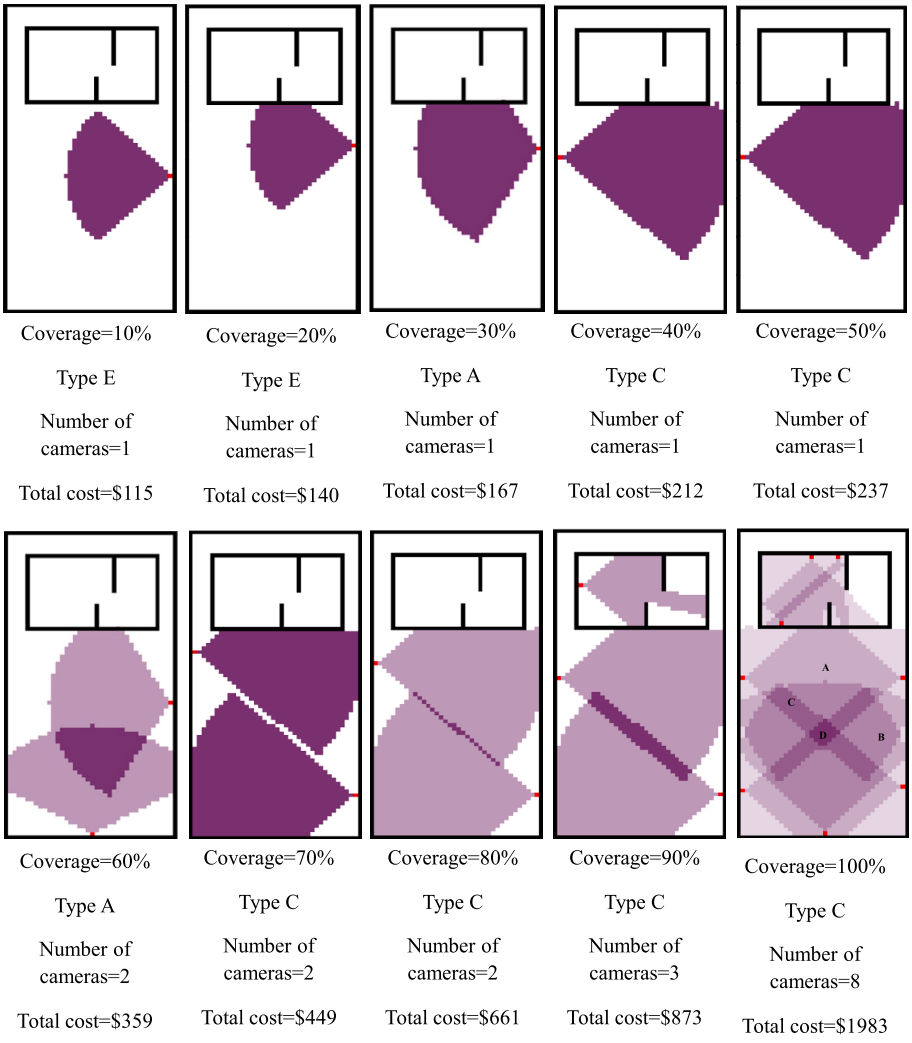

Fig. 12. Optimal camera layout in different scenarios.

in real life due to aspects like power supply, network connectivity, problems associated with access control, and weather protection measures.

This research is conducted based on a case study to achieve the coverage rate of the monitoring environment with an overall coverage of 90 %. The analysis presented in Fig. 11 shows that the C-type camera is the optimal camera type for this objective. The optimal layout for deploying C-type cameras at a 90 % coverage rate, as depicted in Fig. 14, is designed for each phase of the project. This design includes a maximum of four cameras, which provide the required coverage. The budget estimated to be spent on purchasing and relocating CCTV cameras at different phases to obtain the optimal design for this site was $873. Fig. 14 clearly shows that the cameras are covering high-risk, medium-risk, and low-risk areas. Notably, areas behind the building that do not require monitoring were excluded from the surveillance system, reflecting a strategic approach to resource allocation.

The study results, as anticipated, indicate a need for adjustments in both the number and placement of surveillance cameras throughout the construction process. To emphasize the necessity of these modifications, the camera layout during the foundation phase of the proposed case study was implemented under the assumption of a static site layout for subsequent phases. In this scenario, the optimal camera layout determined during the foundation phase was maintained across all subsequent stages. Fig. 15 shows the coverage simulation results for this fixed camera placement strategy in subsequent phases of the project.

Although we initially achieved an impressive 90 % camera coverage rate during the framing phase, a notable drop in coverage was observed during the roughing and finishing phases. This emphasizes the need for camera relocation during construction projects. In detail, coverage fell to 50 % in the roughing phase and 56 % in the finishing phase. This decline can be attributed to the obstruction of camera views by structural elements like walls. Figs. 15(b) and 15(c) illustrate this by showing that the addition of walls during these phases completely eliminated surveillance coverage within the building. Moreover, critical areas designated as high risk (Red B and C zones) and medium risk (Orange A zones) during the roughing and finishing phases were not captured by any cameras.

It is worth mentioning that the camera placed on the side of the building did not capture any footage during the roughing and finishing phases. As a result, not only were key safety areas left without monitoring, but a considerable amount of expenditure was also wasted. Creating a layout for each phase of a project guarantees a practical and flexible approach, enabling necessary modifications to the monitoring system as construction advances.

To further support the practical applicability of the proposed method, we evaluated the final cost and relocation decisions across all construction phases. The case study covered four major phases, during which the system dynamically responded to evolving site layouts and changing high-priority zones. Notably, the system autonomously determined the most cost-effective reconfiguration strategy at each

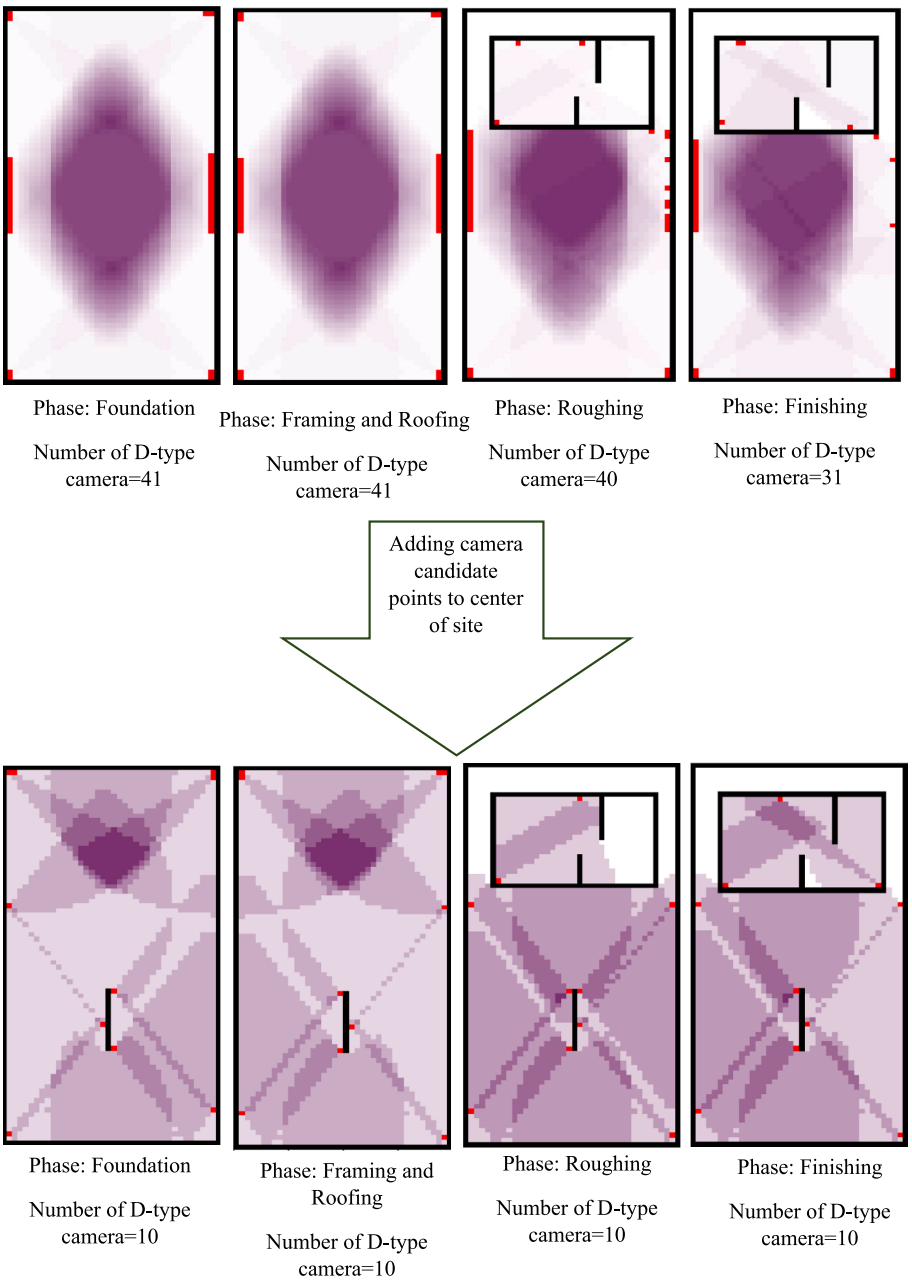

Fig. 13. Optimal camera placement with central candidate point.

transition point. For instance, transitioning from frame and roof works (Phase 2) to roughing works (Phase 3) prompted the relocation of one camera and the addition of another. Similarly, an additional camera was introduced in the transition to finishing works (Phase 4), reflecting the system's adaptive behavior in maintaining adequate coverage over the high-priority zones.

The total monitoring cost across all phases amounted to $873 using the proposed MILP-based approach to achieve at least 90 % coverage throughout all construction phases, compared to $1060 in a static deployment strategy without intelligent relocation. This represents a 17.64 % reduction in total cost, demonstrating that the model not only produces optimal configurations at each phase but also considerably reduces financial overhead. These results validate the model's ability to generate efficient, dynamic surveillance strategies under realistic project constraints and emphasize its value as a practical decision-support tool in construction monitoring.

6. Discussion

To comprehensively evaluate the novelty and practical contributions of the proposed approach, a detailed comparative analysis has been performed against a broad range of existing literature on surveillance camera placement. This evaluation not only illustrates the model's advancements within the construction domain but also emphasizes its applicability across a variety of surveillance environments, including bridges, metro systems, urban areas, and general indoor environments.

The comparison presented in Table 7 is structured according to several evaluation metrics, including dynamic modeling capability, consideration of relocation costs, risk-based prioritization, guarantee of global optimality, availability of open-source code, the type of case study used, and the scale of the case study in square meters.

Table 7 summarizes the comparative analysis of the present study against existing works, highlighting the key differentiating factors. Unlike previous studies, the proposed model systematically incorporates

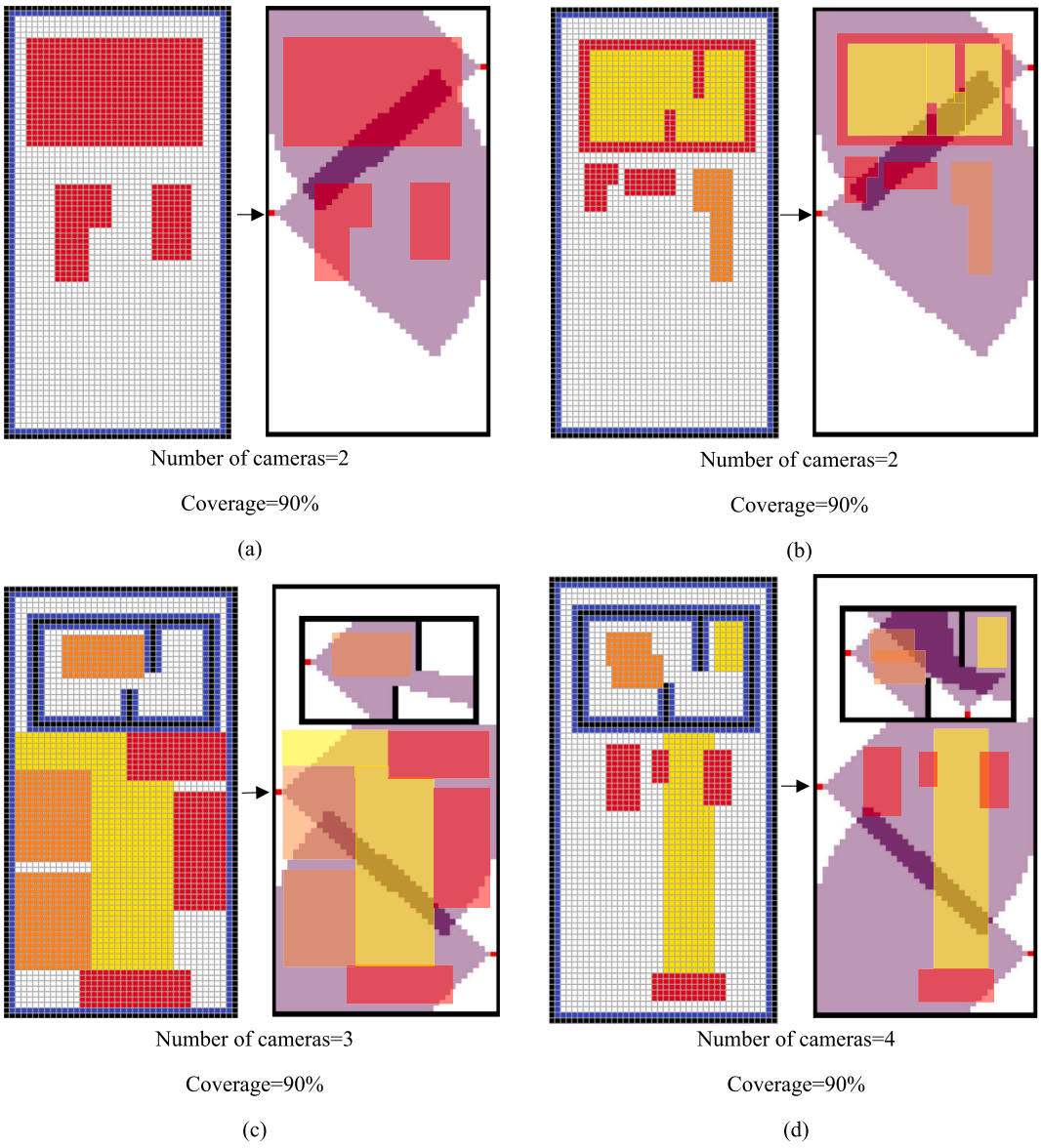

Fig. 14. Optimal camera layout for different phases of the project: (a) Foundation phase; (b) Frame and roof phase; (c) Roughing phase; (d) Finishing phase.

construction site dynamics, relocation costs, and risk-based prioritization within an integrated optimization framework, which is solved using an exact algorithm to ensure global optimality. As seen in the table, most prior research either neglects site evolution or justifies static placements due to high relocation costs. Furthermore, while both heuristic and metaheuristic methods offer faster computational efficiency, they do so at the cost of solution accuracy, leading to potentially suboptimal camera placements and higher long-term costs. The presented model ensures an exact, cost-minimizing surveillance strategy that dynamically adapts to project phases, balancing new camera purchases with relocation decisions. Additionally, this study is among the few that provides open-source code availability, allowing researchers and practitioners to customize and further develop the model based on their specific needs.

By addressing these overlooked aspects, the proposed approach offers a more realistic and practical solution to construction site surveillance, ensuring that camera placements remain cost-effective and adaptable throughout the project lifecycle. A detailed explanation of these contributions is provided below.

1. **Dynamic Model and Relocation Costs**

Construction projects require frequent reassessment of camera placement due to evolving site layouts, risk profiles, and operational constraints. Unlike traditional static methods, the proposed model offers a cost-effective and adaptable surveillance strategy by incorporating relocation and removal costs into the optimization process. As demonstrated in Table 7, previous studies—including various domains such as construction sites, bridges, metros, urban areas, and indoor environments—lack an integrated framework that explicitly addresses dynamic site conditions and their impact on surveillance efficiency and cost. The presented approach fills this gap through an integrated model that accounts for both the evolving nature of the site and the associated relocation costs.

Existing research on camera placement optimization, while sometimes acknowledging site dynamics [9,86], often falls short by neglecting inter-phase continuity and the crucial trade-off between relocation costs and the purchase of new cameras. Instead of optimizing camera

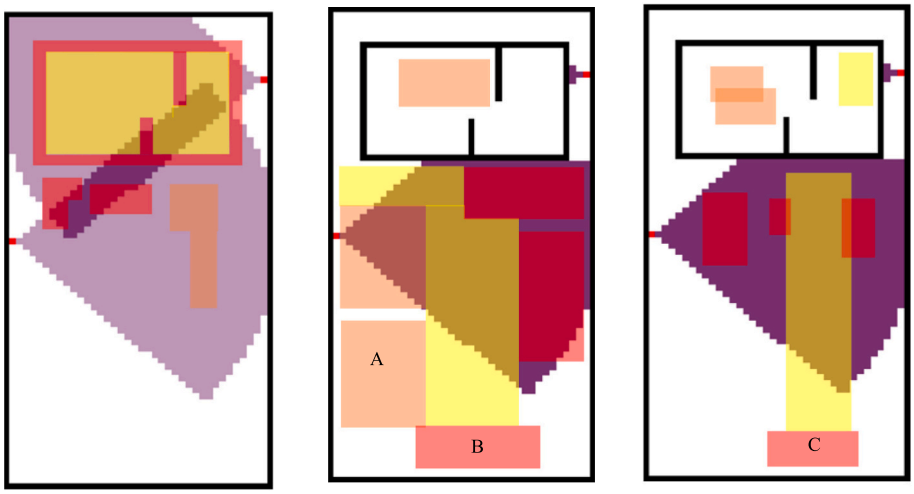

Fig. 15. Optimal layout of the foundation phase in: (a) Framing phase; (b) Rough work phase; (c) Finishing phase.

Table 7
Comparison of the proposed model with related works.

Reference	Methodology	Dynamic Model	Relocation Costs	Risk-Based Prioritization	Global Optimality Guarantee	Open-Source Code Availability	Type of Case Study	Size of Case Study (m2)
[86]	PMGA	×	×	×	×	×	real	2000
[84]	NSGA-II	×	×	✓	×	✓	real	6000
[83]	MIP	×	×	×	×	×	real	13,450
[9]	NSGA-II	×	×	×	×	×	real	3265
[18]	Modified Genetic Algorithm	×	×	×	×	×	real	6560
[85]	GA	×	×	✓	×	×	real	350
[14]	GA	×	×	✓	×	×	real	2100
[87]	COLSA	×	×	✓	×	×	simulation	250,000
[88]	GA	×	×	✓	×	×	real	8500
[98]	Hill Climbing	×	×	×	×	×	simulation	40,000
[90]	BCO	×	×	×	×	×	simulation	N/A
[91]	LH-RPSO (PSO + Resampling + LHS)	×	×	×	×	×	real	83,322
[99]	Greedy, Dual Sampling	×	×	✓	×	×	simulation	N/A
[100]	BPSO	×	×	×	×	×	simulation	400
[101]	BIP	×	×	×	✓	×	simulation	72
[102]	BIP، Greedy، MCMC، SDP	×	×	×	×	×	simulation	N/A
[103]	IP	×	×	×	×	×	real	100
[104]	BIP	×	×	✓	×	×	real	300
[105]	BPSO	×	×	×	×	×	simulation	2250
[80]	Hill-Climbing	×	×	✓	×	×	real	N/A
[106]	GA	×	×	✓	×	×	real	167
[92]	ILP	×	×	✓	×	×	real	132,400
This study	MILP	✓	✓	✓	✓	✓	real	3200

placement across all project phases simultaneously, these studies typically analyze each site plan independently, resulting in phase-specific optimal layouts that fail to consider the overall project trajectory. Moreover, these studies frequently justify maintaining fixed camera positions throughout the project by citing high relocation costs. This leads them to prioritize a single, although suboptimal, camera configuration that performs relatively well across all phases, rather than pursuing phase-specific optimal solutions. This approach neglects the potential benefits of dynamic camera repositioning and ultimately compromises the overall surveillance effectiveness across the project lifecycle.

This lack of a holistic perspective leads to several inefficiencies. First, independently optimizing each phase disregards the potential cost savings and performance gains achievable through strategic camera repositioning. Second, neglecting relocation costs in the optimization process can result in frequent and unnecessary camera movements, increasing project expenses and potentially compromising site safety due to inadequate monitoring adjustments. For example, an apparently optimal placement in one phase could be made instantly obsolete by subsequent construction changes, such as a newly constructed wall obstructing the camera's view. This emphasizes the necessary need for a dynamic optimization process that predicts and adapts to evolving site conditions.

In contrast, the proposed method introduces an integrated mathematical model that integrates site dynamics, relocation costs, and the trade-offs between new camera purchases and repositioning existing

ones. By considering all construction phases simultaneously, this model facilitates strategic resource allocation and minimizes unnecessary expenditures. The result is a cost-effective and sustainable approach that ensures required surveillance coverage throughout the entire project lifecycle while enhancing overall project safety.

2. **Risk-Based Prioritization**

A number of existing studies either completely overlook risk-based prioritization or implement simplistic binary classifications, distinguishing only between "high-priority" and "low-priority" areas. This oversimplification fails to capture the diverse levels of risk present in dynamic construction environments. The present study introduces a more enhanced, four-level risk categorization that improves surveillance efficiency:

- High-risk zones (e.g., heavy machinery areas, hazardous operations)
- Medium-risk zones (e.g., active workspaces, high worker activity areas)
- Low-risk zones (e.g., equipment storage, temporary material placement)
- Non-critical zones (e.g., worker rest areas, managerial offices) – requiring no surveillance

By assigning a weight of zero to non-critical areas, the model effectively eliminates redundant coverage, optimizes camera allocation, and considerably reduces overall costs. This detailed approach to risk-based prioritization enhances economic efficiency and aligns closely with real-world safety and security requirements. As demonstrated in Table 7, few studies incorporate risk-based prioritization, and those that do often fail to implement a multi-level system or dynamically adjust risk levels over time.

3. **Global Optimality Guarantee**

A notable feature of this study is its potential to achieve a globally optimal solution—an aspect not commonly addressed in previous research (as shown in Table 7). Previous studies predominantly rely on heuristic and metaheuristic methods (e.g., genetic algorithms, particle swarm optimization, and greedy methods) for their computational efficiency in large-scale problems. However, these approaches sacrifice accuracy for speed, yielding only approximate solutions that often result in redundant camera placements, inefficient cost allocations and surveillance blind spots across multiple project phases.

In contrast, the present study emphasizes cost minimization by formulating the problem as a Mixed-Integer Linear Programming model and solving it using exact optimization methods, rather than relying on faster but less accurate heuristic and metaheuristic approaches. Although both heuristic and metaheuristic methods provide faster computational results, their inability to systematically explore all possible solutions frequently leads to suboptimal configurations—either by deploying redundant cameras that incur unnecessary costs or by leaving certain high-risk areas inadequately monitored. Considering that monitoring costs represent a significant portion of the overall project expenses, any optimization algorithm that overlooks economic efficiency leads to the risk of generating financially unsustainable monitoring strategies.

Among the reviewed studies, one research work [101] provides an exact solution; however, its applicability to real-world construction projects may be limited, as it is based on a small-scale simulated case and does not explicitly account for dynamic site conditions and relocation costs within its optimization framework.

4. **Type and Size of Case Study**

The type and size of a case study are key factors in determining a study's practical relevance, particularly in the complex and dynamic environment of construction sites. The realism of a study directly influences the applicability of its findings, making real-world case studies essential for deriving meaningful and implementable conclusions. The proposed study is based on a 3200 m^2 real-world construction project, ensuring practical alignment with real project conditions.

While some studies [87,98] utilize large case studies, their reliance on simulated environments limits the generalizability of their findings to real-world scenarios. Furthermore, a number of studies [14,85,86,100,103–106] have employed heuristic and metaheuristic methods that operate on considerably smaller case studies, ranging from 100 to 2250 m^2. While the computational efficiency of these approaches is often cited as justification for their use in large-scale problems, the case studies employed in these instances remain smaller than the one presented in this work. This discrepancy highlights the contribution of this study in applying an exact solution method to a larger, real-world case study.

Although [101] provides an exact solution, as previously noted, it relies on a highly simplified, simulated environment of only 72 m^2, which limits its applicability to real-world scenarios. On the other hand, some studies [9,83,84,88,91,92] attempt to address large-scale, real-world environments, but they often neglect key considerations such as solution exactness, construction phase dynamics, and camera relocation costs. In addition to these limitations, all of the mentioned studies fail to incorporate the dynamic nature of construction and the costs associated with camera relocation within their mathematical models—factors that notably weaken their real-world impact.

In summary, the proposed model represents an integrated, cost-conscious, and phase-adaptive solution for optimizing camera placement in dynamic construction environments. Unlike prior studies that address only a subset of practical requirements, the method simultaneously incorporates site dynamics, relocation costs, prioritized risk zones, and exact optimization guarantees into a single, flexible framework. It is important to emphasize that collecting real-world construction site data is challenging due to access restrictions, privacy concerns, and project management approvals. Moreover, extending to significantly larger case studies would require additional computational resources, which are beyond our current capacity. This open-access approach enables the generation of results that are tailored to the specific demands of distinct projects and the computational resources accessible to researchers.

7. **Conclusions**

Ensuring efficient visual monitoring on construction sites is important to both operational efficiency and safety. However, optimally placing surveillance cameras remains challenging due to the dynamic nature of construction environments and the lack of systematic guidelines. To address these challenges, this paper presented a Mixed-Integer Linear Programming (*MILP*) model for optimizing surveillance camera placement in dynamic construction environments, accounting for the unique characteristics and key factors influencing optimal camera placement.

The proposed framework overcomes the limitations of previous research by simultaneously considering a broader range of factors. Unlike most existing studies, this model provides a global solution rather than relying on approximate algorithms to solve the optimization problem. As a result, it guarantees that the selected locations minimize costs. The model not only reduces the number of cameras required but

also minimizes the costs associated with relocating cameras (installation and removal) between different phases, which arise from the dynamic adjustment of their positions in response to changing site layouts and environmental factors. By generating an optimal layout based on the desired coverage percentage set by the project manager, the model ensures that surveillance needs are precisely met according to the requirements of the project manager.

In this study, the viewing distance of the camera, one of the key variables of the model, is determined based on the objectives of the project manager. For example, if the goal is to identify the type of activity, the number and placement of cameras will differ from when the objective is to identify individual workers. When the goal is to identify individuals, the viewing distance of the camera must be reduced, which in turn increases the number of cameras required. This approach improves the efficiency of the surveillance system by tailoring it to real-world conditions and specific monitoring needs.

This strategy for surveillance involves adjusting camera viewing distances according to the surveillance objectives of the project manager. For instance, if the goal is to identify activities, cameras will be positioned differently than if the goal is to recognize individual workers. This adjustment in viewing distance requires an increase in the number of cameras, thereby enhancing the efficiency of the system and better aligning it with real-world conditions.

The applicability and effectiveness of the proposed framework are verified through an experiment conducted on a 3200-square-meter construction site. The results demonstrate the practical value of the MILP model in optimizing surveillance camera placement and ensuring required coverage while minimizing costs in a dynamic construction environment. The findings highlight the ability of the model to generate optimal camera layouts, balancing cost minimization with the required coverage tailored to the desired level of surveillance defined by the project manager.

Future research should explore the extension of monitoring strategies into three-dimensional environments. Construction sites often involve high-risk activities at various elevations, and traditional two-dimensional surveillance systems may fail to capture vertical dynamics, leading to missed critical zones. Developing 3D-aware monitoring approaches would offer more accurate and comprehensive coverage of hazardous areas, thus enhancing on-site safety.

Another important direction is determining the optimal timing for adjusting camera placements. Due to the dynamic and evolving nature of construction projects, a static camera layout can become inefficient as the site progresses. Identifying suitable intervals for repositioning cameras can ensure sustained monitoring effectiveness and also reduce unnecessary operational adjustments, thereby lowering long-term costs.

Integrating intelligent and digital technologies presents additional opportunities to improve system flexibility. The use of Building Information Modeling (BIM), IoT-enabled sensors, and digital monitoring platforms can support real-time data collection, automated hazard identification, and dynamic adaptation of the surveillance strategy based on live site conditions.

Finally, enhancing the model with a Target Detail Level (TDL) parameter would allow for simultaneous optimization of multiple surveillance objectives—such as detection, recognition, and identification—tailored to different risk zones across the construction site. This would enable hybrid monitoring strategies where certain areas prioritize broader coverage, while others require more detailed visibility. Achieving this would involve expanding the current formulation to incorporate varying field-of-view (FOV) requirements across different site areas.

In conclusion, addressing these future research directions will lead to more effective and efficient surveillance systems for construction sites. The implementation of three-dimensional monitoring, optimized camera arrangements, integration with intelligent technologies, and Field of View (*FOV*) components will contribute to safer construction environments and more cost-effective surveillance practices.

CRediT authorship contribution statement

Mohadeseh Farkhondeh: Writing – original draft, Software, Methodology, Investigation, Formal analysis, Data curation. **Mojtaba Maghrebi:** Writing – original draft, Supervision, Project administration, Methodology, Investigation, Formal analysis.

Declaration of competing interest

The authors declare that they have no known competing financial interests or personal relationships that could have appeared to influence the work reported in this paper.

Data availability

To promote transparency and facilitate further research, the complete methodological framework, source code, and dataset have been made publicly available via GitHub at: *https://github.com/smartconstruction-group/Camera_Placement_Optimization* .This repository enables other researchers to replicate, adapt, and extend the model based on their computational capabilities and site-specific requirements.

References

[1] I.G. Awolusi, E.D. Marks, Safety activity analysis framework to evaluate safety performance in construction, J. Constr. Eng. Manag. 143 (3) (2017) 05016022, https://doi.org/10.1061/(ASCE)CO.1943-7862.0001265.
[2] S. Winge, E. Albrechtsen, B.A. Mostue, Causal factors and connections in construction accidents, Saf. Sci. 112 (2019) 130–141, https://doi.org/10.1016/j.ssci.2018.10.015.
[3] M. Pillay, Accident causation, prevention and safety management: a review of the state-of-the-art, Procedia Manufact. 3 (2015) 1838–1845, https://doi.org/10.1016/j.promfg.2015.07.224.
[4] Commonly Used Statistics | Occupational Safety and Health Administration, n. d. (accessed, 2025) https://www.osha.gov/data/commonstats.
[5] Ministry of Employment and Labor, n. d. (accessed, 2025) https://www.moel.go.kr/english/main.jsp.
[6] J. Garrett, J. Teizer, Human factors analysis classification system relating to human error awareness taxonomy in construction safety, J. Constr. Eng. Manag. 135 (8) (2009) 754–763, https://doi.org/10.1061/(ASCE)CO.1943-7862.0000034.
[7] Y. Yu, H. Guo, Q. Ding, H. Li, M. Skitmore, An experimental study of real-time identification of construction workers' unsafe behaviors, Autom. Constr. 82 (2017) 193–206, https://doi.org/10.1016/j.autcon.2017.05.002.
[8] L. Ding, W. Fang, H. Luo, P.E. Love, B. Zhong, X. Ouyang, A deep hybrid learning model to detect unsafe behavior: integrating convolution neural networks and long short-term memory, Autom. Constr. 86 (2018) 118–124, https://doi.org/10.1016/j.autcon.2017.11.002.
[9] S.V.-T. Tran, T.L. Nguyen, H.-L. Chi, D. Lee, C. Park, Generative planning for construction safety surveillance camera installation in 4D BIM environment, Autom. Constr. 134 (2022) 104103, https://doi.org/10.1016/j.autcon.2021.104103.
[10] E. Rezazadeh Azar, S. Dickinson, B. McCabe, Server-customer interaction tracker: computer vision–based system to estimate dirt-loading cycles, J. Constr. Eng. Manag. 139 (7) (2013) 785–794, https://doi.org/10.1061/(ASCE)CO.1943-7862.0000652.
[11] M. Bügler, A. Borrmann, G. Ogunmakin, P.A. Vela, J. Teizer, Fusion of photogrammetry and video analysis for productivity assessment of earthwork processes, Comput. Aided Civ. Inf. Eng. 32 (2) (2017) 107–123, https://doi.org/10.1111/mice.12235.
[12] Z. Zhu, X. Ren, Z. Chen, Integrated detection and tracking of workforce and equipment from construction jobsite videos, Autom. Constr. 81 (2017) 161–171, https://doi.org/10.1016/j.autcon.2017.05.005.
[13] R. Yaagoubi, M. El Yarmani, A. Kamel, W. Khemiri, HybVOR: a voronoi-based 3D GIS approach for camera surveillance network placement, ISPRS Int. J. Geo Inf. 4 (2) (2015) 754–782, https://doi.org/10.3390/ijgi4020754.
[14] J. Kim, Y. Ham, Y. Chung, S. Chi, Systematic camera placement framework for operation-level visual monitoring on construction jobsites, J. Constr. Eng. Manag. 145 (4) (2019) 04019019, https://doi.org/10.1061/(ASCE)CO.1943-7862.0001636.
[15] J.S. Bohn, J. Teizer, Benefits and barriers of construction project monitoring using high-resolution automated cameras, J. Constr. Eng. Manag. 136 (6) (2010) 632–640, https://doi.org/10.1061/(ASCE)CO.1943-7862.0000164.
[16] Y.-C. Hsieh, Y.-C. Lee, P.-S. You, The optimal locations of surveillance cameras on straight lanes, Expert Syst. Appl. 38 (5) (2011) 5416–5422, https://doi.org/10.1016/j.eswa.2010.10.014.

[17] R. Cole, M. Sharir, Visibility problems for polyhedral terrains, J. Symb. Comput. 7 (1) (1989) 11–30, https://doi.org/10.1016/S0747-7171(89)80003-3.
[18] Y. Zhang, H. Luo, M. Skitmore, Q. Li, B. Zhong, Optimal camera placement for monitoring safety in metro station construction work, J. Constr. Eng. Manag. 145 (1) (2019) 04018118, https://doi.org/10.1061/(ASCE)CO.1943-7862.000158.
[19] U.M. Erdem, S. Sclaroff, Automated placement of cameras in a floorplan to satisfy task-specific constraints, in: *Boston University, Boston December*, vol. 2003, 2003, https://doi.org/10.1016/j.cviu.2006.06.005.
[20] Q. Fang, H. Li, X. Luo, L. Ding, H. Luo, T.M. Rose, W. An, Detecting non-hardhat-use by a deep learning method from far-field surveillance videos, Autom. Constr. 85 (2018) 1–9, https://doi.org/10.1016/j.autcon.2017.09.018.
[21] B.E. Mneymneh, M. Abbas, H. Khoury, Vision-based framework for intelligent monitoring of hardhat wearing on construction sites, J. Comput. Civ. Eng. 33 (2) (2019) 04018066, https://doi.org/10.1061/(ASCE)CP.1943-5487.0000813.
[22] M.-W. Park, N. Elsafty, Z. Zhu, Hardhat-wearing detection for enhancing on-site safety of construction workers, J. Constr. Eng. Manag. 141 (9) (2015) 04015024, https://doi.org/10.1061/(ASCE)CO.1943-7862.0000974.
[23] H. Wu, J. Zhao, An intelligent vision-based approach for helmet identification for work safety, Comput. Ind. 100 (2018) 267–277, https://doi.org/10.1016/j.compind.2018.03.037.
[24] W. Fang, L. Ding, H. Luo, P.E. Love, Falls from heights: a computer vision-based approach for safety harness detection, Autom. Constr. 91 (2018) 53–61, https://doi.org/10.1016/j.autcon.2018.02.018.
[25] Q. Fang, H. Li, X. Luo, L. Ding, H. Luo, C. Li, Computer vision aided inspection on falling prevention measures for steeplejacks in an aerial environment, Autom. Constr. 93 (2018) 148–164, https://doi.org/10.1016/j.autcon.2018.05.022.
[26] Z. Kolar, H. Chen, X. Luo, Transfer learning and deep convolutional neural networks for safety guardrail detection in 2D images, Autom. Constr. 89 (2018) 58–70, https://doi.org/10.1016/j.autcon.2018.01.003.
[27] A. Perlman, R. Sacks, R. Barak, Hazard recognition and risk perception in construction, Saf. Sci. 64 (2014) 22–31, https://doi.org/10.1016/j.ssci.2013.11.019.
[28] Y.J. Cha, W. Choi, O. Büyüköztürk, Deep learning-based crack damage detection using convolutional neural networks, Comput. Aided Civ. Inf. Eng. 32 (5) (2017) 361–378, https://doi.org/10.1111/mice.12263.
[29] S. Han, S. Lee, A vision-based motion capture and recognition framework for behavior-based safety management, Autom. Constr. 35 (2013) 131–141, https://doi.org/10.1016/j.autcon.2013.05.001.
[30] H. Guo, Y. Yu, Q. Ding, M. Skitmore, Image-and-skeleton-based parameterized approach to real-time identification of construction workers' unsafe behaviors, J. Constr. Eng. Manag. 144 (6) (2018) 04018042, https://doi.org/10.1061/(ASCE)CO.1943-7862.0001497.
[31] S. Han, S. Lee, F. Peña-Mora, Vision-based detection of unsafe actions of a construction worker: case study of ladder climbing, J. Comput. Civ. Eng. 27 (6) (2013) 635–644, https://doi.org/10.1061/(ASCE)CP.1943-5487.0000279.
[32] H. Chen, X. Luo, Z. Zheng, J. Ke, A proactive workers' safety risk evaluation framework based on position and posture data fusion, Autom. Constr. 98 (2019) 275–288, https://doi.org/10.1016/j.autcon.2018.11.026.
[33] S. Han, S. Lee, F. Peña-Mora, Comparative study of motion features for similarity-based modeling and classification of unsafe actions in construction, J. Comput. Civ. Eng. 28 (5) (2014) A4014005, https://doi.org/10.1061/(ASCE)CP.1943-5487.0000339.
[34] J. Chen, Y. Fang, Y.K. Cho, Real-time 3D crane workspace update using a hybrid visualization approach, J. Comput. Civ. Eng. 31 (5) (2017) 04017049, https://doi.org/10.1061/(ASCE)CP.1943-5487.0000698.
[35] D. Kim, M. Liu, S. Lee, V.R. Kamat, Remote proximity monitoring between mobile construction resources using camera-mounted UAVs, Autom. Constr. 99 (2019) 168–182, https://doi.org/10.1016/j.autcon.2018.12.014.
[36] Z. Zhu, M.-W. Park, C. Koch, M. Soltani, A. Hammad, K. Davari, Predicting movements of onsite workers and mobile equipment for enhancing construction site safety, Autom. Constr. 68 (2016) 95–101, https://doi.org/10.1016/j.autcon.2016.04.009.
[37] H. Kim, K. Kim, H. Kim, Vision-based object-centric safety assessment using fuzzy inference: monitoring struck-by accidents with moving objects, J. Comput. Civ. Eng. 30 (4) (2016) 04015075, https://doi.org/10.1061/(ASCE)CP.1943-5487.0000562.
[38] S. Chi, C.H. Caldas, Image-based safety assessment: automated spatial safety risk identification of earthmoving and surface mining activities, J. Constr. Eng. Manag. 138 (3) (2012) 341–351, https://doi.org/10.1061/(ASCE)CO.1943-7862.0000438.
[39] X. Chen, K. Henrickson, Y. Wang, Kinect-based pedestrian detection for crowded scenes, Comput. Aided Civ. Inf. Eng. 31 (3) (2016) 229–240, https://doi.org/10.1111/mice.12163.
[40] H. Hamledari, B. McCabe, S. Davari, Automated computer vision-based detection of components of under-construction indoor partitions, Autom. Constr. 74 (2017) 78–94, https://doi.org/10.1016/j.autcon.2016.11.009.
[41] M.-W. Park, I. Brilakis, Construction worker detection in video frames for initializing vision trackers, Autom. Constr. 28 (2012) 15–25, https://doi.org/10.1016/j.autcon.2012.06.001.
[42] G. Gualdi, A. Prati, R. Cucchiara, Contextual information and covariance descriptors for people surveillance: an application for safety of construction workers, Eurasip J. Image Video Process. 2011 (2011) 1–16, https://doi.org/10.1155/2011/684819.
[43] K. Ranaweera, J. Ruwanpura, S. Fernando, Automated real-time monitoring system to measure shift production of tunnel construction projects, J. Comput. Civ. Eng. 27 (1) (2013) 68–77, https://doi.org/10.1061/(ASCE)CP.1943-5487.0000199.
[44] E. Rezazadeh Azar, B. McCabe, Automated visual recognition of dump trucks in construction videos, J. Comput. Civ. Eng. 26 (6) (2012) 769–781, https://doi.org/10.1061/(ASCE)CP.1943-5487.00001.
[45] J. Teizer, P.A. Vela, Personnel tracking on construction sites using video cameras, Adv. Eng. Inform. 23 (4) (2009) 452–462, https://doi.org/10.1016/j.aei.2009.06.011.
[46] J. Yang, O. Arif, P.A. Vela, J. Teizer, Z. Shi, Tracking multiple workers on construction sites using video cameras, Adv. Eng. Inform. 24 (4) (2010) 428–434, https://doi.org/10.1016/j.aei.2010.06.008.
[47] S.J. Ray, J. Teizer, Real-time construction worker posture analysis for ergonomics training, Adv. Eng. Inform. 26 (2) (2012) 439–455, https://doi.org/10.1016/j.aei.2012.02.011.
[48] X. Yang, Y. Yu, H. Li, X. Luo, F. Wang, Motion-based analysis for construction workers using biomechanical methods, Front. Eng. Manag. 4 (1) (2017) 84–91, https://doi.org/10.15302/J-FEM-2017004.
[49] X. Luo, H. Li, D. Cao, F. Dai, J. Seo, S. Lee, Recognizing diverse construction activities in site images via relevance networks of construction-related objects detected by convolutional neural networks, J. Comput. Civ. Eng. 32 (3) (2018) 04018012, https://doi.org/10.1061/(ASCE)CP.1943-5487.0000756.
[50] X. Luo, H. Li, X. Yang, Y. Yu, D. Cao, Capturing and understanding workers' activities in far-field surveillance videos with deep action recognition and Bayesian nonparametric learning, Comput. Aided Civ. Inf. Eng. 34 (4) (2019) 333–351, https://doi.org/10.1111/mice.12419.
[51] X. Luo, H. Li, D. Cao, Y. Yu, X. Yang, T. Huang, Towards efficient and objective work sampling: recognizing workers' activities in site surveillance videos with two-stream convolutional networks, Autom. Constr. 94 (2018) 360–370, https://doi.org/10.1016/j.autcon.2018.07.011.
[52] Y. Bai, J. Huan, S. Kim, Measuring bridge construction efficiency using the wireless real-time video monitoring system, J. Manag. Eng. 28 (2) (2012) 120–126, https://doi.org/10.1061/(ASCE)ME.1943-5479.0000061.
[53] H. Luo, C. Xiong, W. Fang, P.E. Love, B. Zhang, X. Ouyang, Convolutional neural networks: computer vision-based workforce activity assessment in construction, Autom. Constr. 94 (2018) 282–289, https://doi.org/10.1016/j.autcon.2018.06.007.
[54] M. Golparvar-Fard, A. Heydarian, J.C. Niebles, Vision-based action recognition of earthmoving equipment using spatio-temporal features and support vector machine classifiers, Adv. Eng. Inform. 27 (4) (2013) 652–663, https://doi.org/10.1016/j.aei.2013.09.001.
[55] J. Kim, S. Chi, J. Seo, Interaction analysis for vision-based activity identification of earthmoving excavators and dump trucks, Autom. Constr. 87 (2018) 297–308, https://doi.org/10.1016/j.autcon.2017.12.016.
[56] S. Chi, C.H. Caldas, Automated object identification using optical video cameras on construction sites, Comput. Aided Civ. Inf. Eng. 26 (5) (2011) 368–380, https://doi.org/10.1111/j.1467-8667.2010.00690.x.
[57] I. Brilakis, M.-W. Park, G. Jog, Automated vision tracking of project related entities, Adv. Eng. Inform. 25 (4) (2011) 713–724, https://doi.org/10.1016/j.aei.2011.01.003.
[58] S. Chi, C.H. Caldas, D.Y. Kim, A methodology for object identification and tracking in construction based on spatial modeling and image matching techniques, Comput. Aided Civ. Inf. Eng. 24 (3) (2009) 199–211, https://doi.org/10.1111/j.1467-8667.2008.00580.x.
[59] J. Gong, C.H. Caldas, Computer vision-based video interpretation model for automated productivity analysis of construction operations, J. Comput. Civ. Eng. 24 (3) (2010) 252–263, https://doi.org/10.1061/(ASCE)CP.1943-5487.0000027.
[60] J. Gong, C.H. Caldas, C. Gordon, Learning and classifying actions of construction workers and equipment using bag-of-video-feature-words and Bayesian network models, Adv. Eng. Inform. 25 (4) (2011) 771–782, https://doi.org/10.1016/j.aei.2011.06.002.
[61] Y. Wu, H. Kim, C. Kim, S.H. Han, Object recognition in construction-site images using 3D CAD-based filtering, J. Comput. Civ. Eng. 24 (1) (2010) 56–64, https://doi.org/10.1061/(ASCE)0887-3801(2010)24:1(56).
[62] S. Roh, Z. Aziz, F. Pena-Mora, An object-based 3D walk-through model for interior construction progress monitoring, Autom. Constr. 20 (1) (2011) 66–75, https://doi.org/10.1016/j.autcon.2010.07.003.
[63] X. Zhang, N. Bakis, T.C. Lukins, Y.M. Ibrahim, S. Wu, M. Kagioglou, G.F. Aouad, A.P. Kaka, E. Trucco, Automating progress measurement of construction projects, Autom. Constr. 18 (3) (2009) 294–301, https://doi.org/10.1016/j.autcon.2008.09.004.
[64] H. Son, C. Kim, 3D structural component recognition and modeling method using color and 3D data for construction progress monitoring, Autom. Constr. 19 (7) (2010) 844–854, https://doi.org/10.1016/j.autcon.2010.03.003.
[65] K.K. Han, M. Golparvar-Fard, Appearance-based material classification for monitoring of operation-level construction progress using 4D BIM and site photologs, Autom. Constr. 53 (2015) 44–57, https://doi.org/10.1016/j.autcon.2015.02.007.
[66] A. Dimitrov, M. Golparvar-Fard, Vision-based material recognition for automated monitoring of construction progress and generating building information modeling from unordered site image collections, Adv. Eng. Inform. 28 (1) (2014) 37–49, https://doi.org/10.1016/j.aei.2013.11.002.
[67] Y. Turkan, F. Bosche, C.T. Haas, R. Haas, Automated progress tracking using 4D schedule and 3D sensing technologies, Autom. Constr. 22 (2012) 414–421, https://doi.org/10.1016/j.autcon.2011.10.003.

[68] P. Tang, D. Huber, B. Akinci, Characterization of laser scanners and algorithms for detecting flatness defects on concrete surfaces, J. Comput. Civ. Eng. 25 (1) (2011) 31–42, https://doi.org/10.1061/(ASCE)CP.1943-5487.0000073.
[69] Q. Wang, J.C. Cheng, H. Sohn, Automated estimation of reinforced precast concrete rebar positions using colored laser scan data, Comput. Aided Civ. Inf. Eng. 32 (9) (2017) 787–802, https://doi.org/10.1111/mice.12293.
[70] B. Akinci, F. Boukamp, C. Gordon, D. Huber, C. Lyons, K. Park, A formalism for utilization of sensor systems and integrated project models for active construction quality control, Autom. Constr. 15 (2) (2006) 124–138, https://doi.org/10.1016/j.autcon.2005.01.008.
[71] A. Salem, S. Kabir, A. Musbah, Optical image analysis based concrete damage detection, in: Proceedings of the Progress in Electromagnetics Research Symposium (PIERS), Marrakesh, Morocco, 20–23 March 2011. PIERS 2011 Marrakesh. Volume 1 of 2. ISBN: 978-1-61782-787-7, 2011, pp. 760–763.
[72] C.M. Yeum, S.J. Dyke, Vision-based automated crack detection for bridge inspection, Comput. Aided Civ. Inf. Eng. 30 (10) (2015) 759–770, https://doi.org/10.1111/mice.12141.
[73] Y.J. Cha, W. Choi, G. Suh, S. Mahmoudkhani, O. Büyüköztürk, Autonomous structural visual inspection using region-based deep learning for detecting multiple damage types, Comput. Aided Civ. Inf. Eng. 33 (9) (2018) 731–747, https://doi.org/10.1111/mice.12334.
[74] X. Kong, J. Li, Vision-based fatigue crack detection of steel structures using video feature tracking, Comput. Aided Civ. Inf. Eng. 33 (9) (2018) 783–799, https://doi.org/10.1111/mice.12353.
[75] F.C. Chen, M.R. Jahanshahi, R.T. Wu, C. Joffe, A texture-based video processing methodology using Bayesian data fusion for autonomous crack detection on metallic surfaces, Comput. Aided Civ. Inf. Eng. 32 (4) (2017) 271–287, https://doi.org/10.1111/mice.12256.
[76] A.A. Zhang, K.C.P. Wang, B. Li, E. Yang, X. Dai, Y. Peng, Y. Fei, Y. Liu, J.Q. Li, C. Chen, Automated pixel-level pavement crack detection on 3D asphalt surfaces using a deep-learning network, Comput. Aided Civ. Inf. Eng. 32 (10) (2017) 805–819, https://doi.org/10.1111/mice.12297.
[77] J. O'Rourke, Art Gallery Theorems and Algorithms, Oxford University Press, New York, 1987. ISBN: 978–0–19-503965-4.
[78] D. Lee, A. Lin, Computational complexity of art gallery problems, IEEE Trans. Inf. Theory 32 (2) (1986) 276–282, https://doi.org/10.1109/TIT.1986.1057165.
[79] Art gallery and illumination problems, in: J. Urrutia, J. Sack, J. Urrutia (Eds.), Handbook of Computational Geometry, Elsevier, Amsterdam, 2000, pp. 973–1027, https://doi.org/10.1016/B978-044482537-7/50023-1. ISBN: 978-0-444-82537-7.
[80] R. Bodor, A. Drenner, P. Schrater, N. Papanikolopoulos, Optimal camera placement for automated surveillance tasks, J. Intell. Robot. Syst. 50 (2007) 257–295, https://doi.org/10.1007/s10846-007-9164-7.
[81] G. Dagnelie, Visual Prosthetics: Physiology, Bioengineering, Rehabilitation, Springer Science & Business Media, New York, 2011, https://doi.org/10.1007/978-1-4419-0754-7, ISBN: 978-1-4419-0753-0.
[82] K.K.C. Dohse, Effects of Field of View and Stereo Graphics on Memory in Immersive Command and Control, Iowa State University, Ames, IA, Master's thesis, 2007. ISBN: 978-0-549-33503-0.
[83] A.T. Murray, K. Kim, J.W. Davis, R. Machiraju, R. Parent, Coverage optimization to support security monitoring, Comput. Environ. Urban. Syst. 31 (2) (2007) 133–147, https://doi.org/10.1016/j.compenvurbsys.2006.06.002.
[84] X. Yang, H. Li, T. Huang, X. Zhai, F. Wang, C. Wang, Computer-aided optimization of surveillance cameras placement on construction sites, Comput. Aided Civ. Inf. Eng. 33 (12) (2018) 1110–1126, https://doi.org/10.1111/mice.12385.
[85] A.H. Albahri, A. Hammad, Simulation-based optimization of surveillance camera types, number, and placement in buildings using BIM, J. Comput. Civ. Eng. 31 (6) (2017) 04017055, https://doi.org/10.1061/(ASCE)CP.1943-5487.000070.
[86] X. Chen, Y. Zhu, H. Chen, Y. Ouyang, X. Luo, X. Wu, BIM-based optimization of camera placement for indoor construction monitoring considering the construction schedule, Autom. Constr. 130 (2021) 103825, https://doi.org/10.1016/j.autcon.2021.103825.
[87] S. Jun, T.-W. Chang, H. Jeong, S. Lee, Camera placement in smart cities for maximizing weighted coverage with budget limit, IEEE Sensors J. 17 (23) (2017) 7694–7703, https://doi.org/10.1109/JSEN.2017.2723481.
[88] S. Jun, T.-W. Chang, H.-J. Yoon, Placing visual sensors using heuristic algorithms for bridge surveillance, Appl. Sci. 8 (1) (2018) 70, https://doi.org/10.3390/app8010070.
[89] J.-W. Ahn, T.-W. Chang, S.-H. Lee, Y.W. Seo, Two-phase algorithm for optimal camera placement, Sci. Program. 2016 (2016), https://doi.org/10.1155/2016/4801784.
[90] D. Chrysostomou, A. Gasteratos, Optimum multi-camera arrangement using a bee colony algorithm, in: 2012 IEEE International Conference on Imaging Systems and Techniques Proceedings, IEEE, 2012, pp. 387–392, https://doi.org/10.1109/IST.2012.6295580.
[91] X. Wang, H. Zhang, H. Gu, Solving optimal camera placement problems in IoT using LH-RPSO, IEEE Access 8 (2019) 40881–40891, https://doi.org/10.1109/ACCESS.2019.2941069.
[92] Z. Han, S. Li, C. Cui, H. Song, Y. Kong, F. Qin, Camera planning for area surveillance: a new method for coverage inference and optimization using location-based service data, Comput. Environ. Urban. Syst. 78 (2019) 101396, https://doi.org/10.1016/j.compenvurbsys.2019.101396.
[93] H.K. Versteeg, W. Malalasekera, An Introduction to Computational Fluid Dynamics: The Finite *volume method*, Pearson education, 2007.
[94] Video surveillance systems for use in security applications – Part 4: Application guideline, in: International Standard IEC 62676–4:2015, I. E. Commission, 2015.
[95] Python. https://www.python.org/downloads/release/python-3121/, 2023 (accessed 3 October 2023).
[96] Visual Studio Code [Online]. Available: https://code.visualstudio.com/updates/v1_89, 2023.
[97] IBM, "IBM ILOG CPLEX Optimization Studio," Version 22.1.0, IBM Corporation, 2023 [Online]. Available: https://www.ibm.com/products/ilog-cplex-optimization-studio.
[98] J.-W. Ahn, T.-W. Chang, S.-H. Lee, Y.W. Seo, Two-phase algorithm for optimal camera placement, Sci. Program. 2016 (1) (2016) 4801784, https://doi.org/10.1155/2016/4801784.
[99] E. Hörster, R. Lienhart, On the optimal placement of multiple visual sensors, in: Proceedings of the 4th ACM international workshop on Video surveillance and sensor networks, 2006, pp. 111–120, https://doi.org/10.1145/1178782.117880.
[100] Y. Morsly, N. Aouf, M.S. Djouadi, On the optimal placement of multiple visual sensor based binary particle swarm optimization, IFAC Proc. Volumes 42 (19) (2009) 279–285, https://doi.org/10.3182/20090921-3-TR-3005.00050.
[101] J.-J. Gonzalez-Barbosa, T. Garcia-Ramirez, J. Salas, J.-B. Hurtado-Ramos, J.-D.-J. Rico-Jimenez, Optimal camera placement for total coverage, in: 2009 IEEE International Conference on Robotics and Automation, IEEE, 2009, pp. 844–848, https://doi.org/10.1109/ROBOT.2009.5152761.
[102] J. Zhao, R. Yoshida, S.-C.S. Cheung, D. Haws, Approximate techniques in solving optimal camera placement problems, Int. J. Distrib. Sensor Netw. 9 (11) (2013) 241913, https://doi.org/10.1155/2013/241913.
[103] U.M. Erdem, S. Sclaroff, Automated camera layout to satisfy task-specific and floor plan-specific coverage requirements, Comput. Vis. Image Underst. 103 (3) (2006) 156–169, https://doi.org/10.1016/j.cviu.2006.06.005.
[104] Y. Yao, C.-H. Chen, B. Abidi, D. Page, A. Koschan, M. Abidi, Sensor planning for automated and persistent object tracking with multiple cameras, in: 2008 IEEE Conference on Computer Vision and Pattern Recognition, IEEE, 2008, pp. 1–8, https://doi.org/10.1109/CVPR.2008.4587515.
[105] Y. Morsly, N. Aouf, M.S. Djouadi, M. Richardson, Particle swarm optimization inspired probability algorithm for optimal camera network placement, IEEE Sensors J. 12 (5) (2011) 1402–1412, https://doi.org/10.1109/JSEN.2011.2170833.
[106] S. Indu, S. Chaudhury, N.R. Mittal, A. Bhattacharyya, Optimal sensor placement for surveillance of large spaces, in: 2009 Third ACM/IEEE International Conference on Distributed Smart Cameras (ICDSC), IEEE, 2009, pp. 1–8, https://doi.org/10.1109/ICDSC.2009.5289398.